A path towards high efficiency using Argon in an HCCI engine

Thesis by

Abdulrahman Magdy Mohammed

In Partial Fulfillment of the Requirements

For the Degree of Master of Science

King Abdullah University of Science and Technology

Thuwal, Kingdom of Saudi Arabia

November, 2018

EXAMINATION COMMITTEE PAGE

The thesis of Abdulrahman Magdy Mohammed is approved by the examination committee.

Committee Chairperson: Prof. Bengt Johansson

Committee Members:
Prof. Robert Dibble, Prof. Mani Sarathy, Prof. Taous-Meriem Laleg-Kirati

ABSTRACT

A path towards high efficiency using Argon in an HCCI engine

Abdulrahman Magdy Mohammed

Argon replacing nitrogen has been examined as a new engine cycle to reach high efficiency. Experiments were carried out under Homogeneous Charge Compression Ignition (HCCI) conditions using a single cylinder variable compression ratio Cooperative Fuel Research (CFR) engine. Isooctane has been used as the fuel for this study. All the parameters were kept fixed but the compression ratio to make the combustion phasing constant. Typical engine outputs and emissions were compared to conventional cycles with both air and synthetic air. It has been found that the compression ratio of the engine must be significantly reduced while using argon due to its higher specific heat ratio. The resulting in-cylinder pressure was lower but combustion remains aggressive. However, greater in-cylinder temperatures were reached. To an end, argon allows gains in fuel efficiency, in unburned hydrocarbon and carbon monoxide, as well as in indicated efficiency. A higher nitrogen oxide concentration while replacing nitrogen by argon was observed but the origin remains to be identified. The concept should therefore be able to reach zero-NOx emissions as no nitrogen should be present.

ACKNOWLEDGEMENTS

“If ye give thanks, I will give you more” Quran 14:7

All thanks go to Allah. He has blessed me with a beautiful family, a great advisor, and an outstanding laboratory to conduct my work.

No words can express my gratitude to my advisor Prof. Bengt Johansson. He was a friend who pushed me to work and at the same time a professional who teaches you how to work properly. I am also grateful to Dr. Jean-Baptiste Masurier, I consider him as my second advisor and I have learned a lot from him.

This work would not be possible without the immense support I received from my mother who taught me how to love, my father who taught me how to live, and my brothers and sisters who were the application of both!

Finally, I would like to thank my fiancée Tasneem for energizing my life with love, peace, and happiness.

TABLE OF CONTENTS

LIST OF FIGURES

LIST OF TABLES

Chapter 1: Introduction

1.1 Energy demand

Industrial revolution has dramatically changed the way humans are living. Steam engines and later internal combustion engines and gas turbines have changed both the industry and transportation. This has sparked a magnificent growth in world population from only 700 million people at the beginning of the industrial revolution to 7 billion people today. The United Nations foresees that this number will grow to 9.3 billion in 2050 and then it will increase to 10.1 billion in 2100 [1]. Energy demand is thus increasing worldwide to satisfy this high growth. While the global energy demand is rising more slowly compared to trends in the past, it is still rising with higher rates. The international energy agency is estimating that energy demand will increase by 30% between 2017 and 2040 [2]. The U.S. energy information administration (EIA) confirms this estimation and predicts that energy consumption will rise from 575 quadrillion British thermal units in 2015 to 736 quadrillion BTU by 2040 [3]. The energy supply to satisfy this high demand come from three main sources. Those are nuclear power plants, renewables, and fossil fuels.

Nuclear energy is a relatively cheap energy source and at the same time could ensure the mitigation of the climate change by reducing CO_2 emissions [4]. But because of its hazardous waste and the extreme severity of its accidents, nuclear energy is not growing as expected for a relatively clean energy source. People still believe that it is not safe enough to have a nuclear power plant and this affects politicians' decisions to build such plants. On top of that, the Fukushima nuclear disaster that happened on March 11, 2011 has increased those fears. For example, the risk perception of residents near a nuclear power plant in china has almost doubled after the Fukushima disaster [5]. Thus, The EIA estimates that nuclear energy will satisfy less than 5% of the world energy demand by 2040. This translates to around 40 billion BTU [3].

There are many ongoing research projects to increase the viability of renewables. Also, many countries are starting to invest in renewable energy. Approximately 98 gigawatts of solar power was installed worldwide in 2017. This represents around 38% of the net energy generation added in that year including renewables, nuclear, and fossil fuels [6]. Today, the world relies on renewables to generate around 12% of its electricity demand and this saved approximately 1.8 gigatonnes of CO_2 [6]. However, despite the ambitions that renewables may be the main energy source in the future, there is still a lot of technological and logistic barriers that has to be considered. Hansen et al. argue that

there is a growing gap between the expressed ambitions and the actual growth rate of renewables based on the present data [7]. The aforementioned energy outlook by EIA predicts that renewables will represent fifth of the energy resources by 2040 [3].

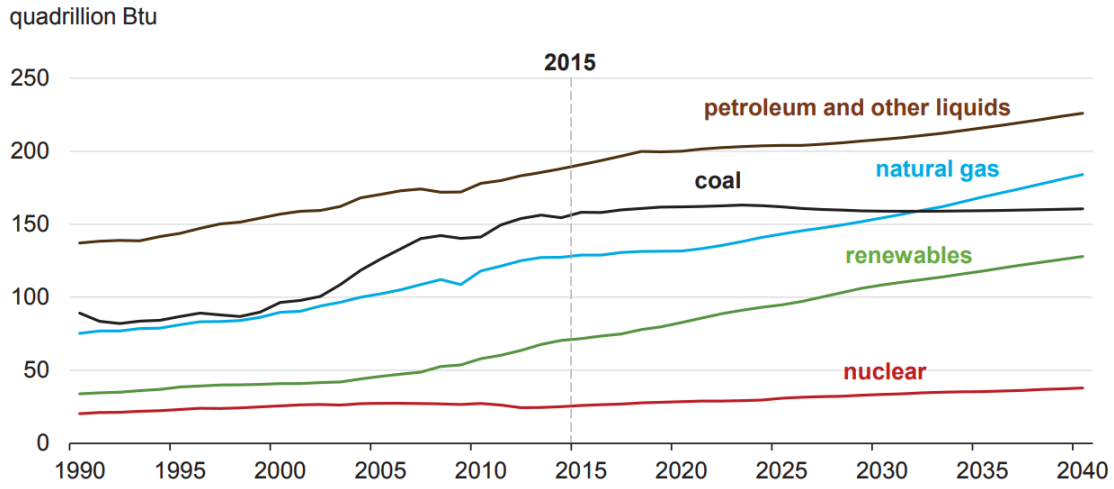

Figure 1: World energy consumption by energy source [3]

Fossil fuels remain the major energy source especially for the transportation sector [8]. Internal combustion engines (ICE) is probably the most common mechanical machine in the world and any efficiency improvement no matter how small will result in less fuel consumption and hence less CO_2 emissions.

1.2 Internal combustion engine efficiency

The purpose of the internal combustion engines is to convert the chemical energy stored in the fuel into useful mechanical work. The efficiency of this process is known as fuel efficiency, fuel economy, or simply brake engine efficiency. A quick overview of appendix B will reveal that engine efficiency depends on four different efficiencies: combustion efficiency, thermodynamic efficiency, gas exchange efficiency, and finally mechanical efficiency.

Thermodynamic efficiency has limited the overall engine efficiency because of limitations imposed by the Carnot cycle and also excessive heat transfer losses. Many thermodynamic cycles can be utilized to model the combustion process inside the engine. Otto cycle is probably the most famous and easy-to-prehend model. Preliminary examination of this model shows that the thermodynamic efficiency of the engine depends on two parameters the volume compression ratio R_c and the specific heat ratio γ. It is worth noting here that this model is ideal and assumes constant volume heat addition at TDC with isentropic compression and expansion processes. Equation 1 shows the thermodynamic efficiency based on Otto cycle.

$$\eta_{th} = 1 - \frac{1}{R_c^{\gamma-1}} \quad (1)$$

Equation 1 shows that increasing either R_c or γ is expected to increase the engine thermodynamic efficiency. Thus, design concepts aiming to increase engine efficiency could be divided into two different categories, either increasing R_c or γ.

1.2.1 Increasing compression ratio

Assuming a specific heat ratio of 1.3, increasing the compression ratio to 60:1 will result in increasing the thermodynamic efficiency to 70% but this is not the whole story. Increasing the compression ratio will result in knock that is detrimental to the engine. Furthermore, higher in-cylinder pressure and temperature catalyzing significant heat transfer losses. Figure 2 demonstrates this behavior utilizing the heat transfer model proposed by Woschni [9].

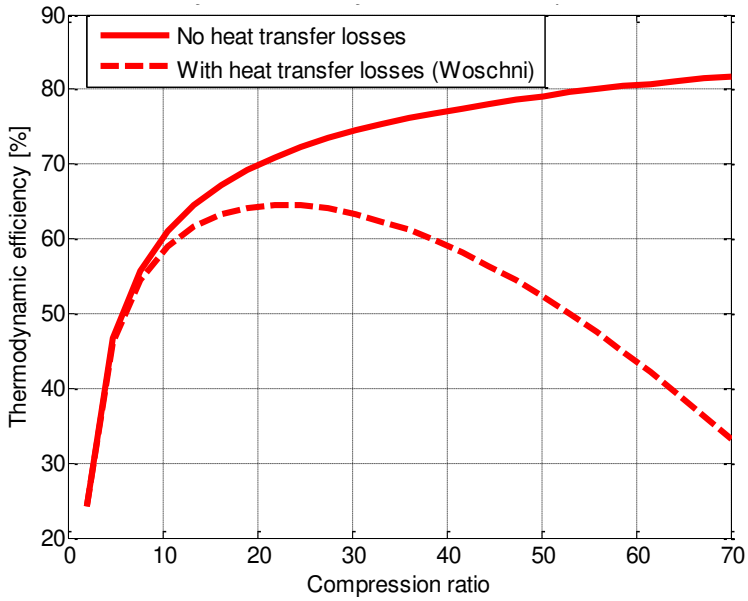

Figure 2: Effect of heat transfer losses on engine thermodynamic efficiency as a function of compression ratio (Retrieved from Bengt Johansson's High efficiency lecture)

Boosting efficiency by combined compression ratios has been studied by a group of researchers in Lund University. Computer simulations for their concept has shown a dramatic improvement in thermodynamic efficiency to be in order of 60% [10].

1.2.2 Increasing the specific heat ratio

Another way to increase the thermodynamic efficiency is to have a working media with higher specific heat ratio. Argon gas has the highest possible specific heat ratio since it is

a monoatomic gas. It is the perfect candidate for this purpose because of its low price compared to other monoatomic gases. This is due to its availability representing almost 0.93% of the atmospheric air.

Diluting the intake air with a noble gas is expected to increase the thermodynamic efficiency. Moneib et al. have shown a better brake thermal efficiency with slightly higher CO emissions and acceptable NOx emissions when diluting the intake air with argon in a spark ignited gasoline engine [11]. Similar results from a Stoichiometric Natural Gas Engine have been published by Li et al in SI combustion mode [12].

Furthermore, using hydrogen as fuel will eliminate the CO2 emissions. This is not a recent idea and it is probably as old as the internal combustion engine itself. Cecil in 1822 used hydrogen as fuel for his vacuum internal combustion engine [13]. Boer et al. in 1978 have shown the practicality of the hydrogen engine in terms of its performance since it has higher specific heat ratio compared to gasoline and this increases its thermodynamic efficiency [14]. One problem with hydrogen fuel is its lower density compared to liquid fuels. This means that larger storage units is needed for such engines which is a problem especially for vehicles. Researchers from Musashi institute of technology in Japan has developed a car that runs on liquid hydrogen and they have shown an increased fuel economy and lower emissions [15].

While the hydrogen engine eliminates CO2 and CO emissions, it still has the problem of high NOx formation due to the high in-cylinder temperature. Oxy-fuel combustion could be a solution to that problem since this will eliminate nitrogen in the system. Results for oxy-fuel combustion using normal gasoline in SI engines are already published to eliminate the NOx emissions and simplify the engine after-treatment system. Wu eta al. were able to increase the indicated thermal efficiency from 32.1% to 41.5% by oxy-fuel combustion with direct water injection to moderate the peak in-cylinder temperature and increase the mass of working gas inside the cylinder [16]. Similar experiment has been also done by Kang et al. in HCCI mode to study the stability of oxy-fuel combustion with direct water injection [17].

Oxy-fuel combustion with hydrogen as fuel increases the in-cylinder temperature to unacceptable limits. For this reason, the engine is operated very rich with more hydrogen to decrease the adiabatic flame temperature. A model developed by Li and Karim [18] predicted efficiency increase when this idea is implemented in spark-ignited engines. Simulations for Hydrogen-oxygen combustion in Diesel-like compression ignition engines have also shown increased efficiency with water injection and excessive steam as residual gases [19].

The idea of increasing the thermodynamic efficiency by a high specific heat ratio oxidizer and hydrogen as fuel was introduced by Lauman and Reynolds in 1976 [20]. This way the combustion products will be only water that can be condensed and argon that is rerouted back to the intake and mixed with argon and no exhaust pipe is needed. This concept was tested by Boer and Hulet and they have proven a significant efficiency increase when the noble gas concentrations are above 75% [21].

Toyota Corporation evaluated the possibility of having a compact vehicle engine that runs on hydrogen as fuel and argon/oxygen mixture as the oxidant. Since they recirculated the exhaust gases, the only problem they faced is the accumulation of CO_2 as a result of lubricating oil combustion. However, their proposed concept showed a dramatic improvement in efficiency [22]. Also, experiments on the same concept have been conducted by Killingsworth et al. Their results showed an increment of the indicated thermal efficiency from approximately 36% in the case of air to around 44% when air is replaced by argon/oxygen mixture [23]. A problem associated with the argon power cycle is that the elevated temperature inside the engine cylinder increases the possibility of engine knock. A possible solution is to regulate the heat release rate inside the combustion chamber by direct fuel injection [24].

Simulations have been conducted by Hafiz et al. to study the effect of hydrogen combustion in argon/oxygen mixture in terms of in-cylinder pressure, in-cylinder temperatures, and heat release rates [25]. To the author's knowledge, the work of this thesis is the first in engine community to study the feasibility of the argon engine in HCCI combustion mode.

The following chapters introduce the methodology and experimental setup used to evaluate the concept of increasing efficiency using argon in HCCI engines. This is followed by results discussion. The thesis is then concluded by the main observations and future work.

Chapter 2: Methodology and Experimental Setup

Replacing the internal combustion engine working media with a medium with higher specific heat ratio is expected to increase the thermodynamic efficiency and also reduce the unburned hydrocarbons because of the elevated in-cylinder temperature. For this purpose an HCCI engine was ran in three modes, the first reference case is with isooctane and air as the oxidizer. The second case was with the air replaced by oxygen and nitrogen from gas supplies. The third case was with the same air and oxygen fuel rates to the engine but replacing the nitrogen with argon. The engine was not operated with recycling of the argon and hence the operating time of the engine had to be limited due to significant argon consumption rate. Exhaust analysis was conducted using an FTIR emission analyzer. This chapter begins by details about the experimental approach and then discusses the experimental setup along with the equipment utilized.

2.1 Methodology

An experimental approach was followed to assist the viability of having an argon HCCI engine. Any fuel could be used for this assessment since the cases are compared to each other. However, Isooctane was chosen to avoid any knocking possibility especially with the severe combustion caused by the expected increase in temperature when the argon mixture is used.

As highlighted in the introduction, three different oxidizer mixtures were used. Air was chosen as the reference mixture. The second mixture is synthetic air in which nitrogen and oxygen were mixed in volume percentages of 80% and 20%, respectively. The main purpose of running this mixture is to make sure that the proposed method of partial pressure mixing is working properly and not deviating much from the ideal gas behavior. More details about this partial fraction mixing is presented in the next experimental setup section. The third oxidizer mixture was made of 80% argon and 20% oxygen by volume. Table 1 summarizes the aforementioned oxidizers compositions.

Table 1: Oxidizers used in the experiments and their compositions

Oxidizer mixtures	O_2 (%)	N_2 (%)	Ar (%)
Compressed Air	20.95	78.09	0.93
Synthetic air	20.0	80.0	0.0
Argon + Oxygen	20.0	0.0	80.0

It was found that the best combustion stability was achieved when phasing the combustion with CA50 at TDC and operating at an equivalence ratio of 0.4. The equivalence ratio (ϕ) could be ambiguous when using the argon mixture because the formal definition is that ϕ is the mass fuel/air ratio relative the stoichiometric composition. To avoid this confusion, any reference to the equivalence ratio in this thesis means the actual fuel/oxygen ratio relative to the stoichiometric one.

An idea proposed by professor Dibble [26] is to burn hydrogen as fuel with Ar/O2 mixture as an oxidizer. The combustion products will be water that can be condensed and argon is routed back to the intake. Alternatively, it has been decided to run the engine with an open loop in which isooctane is combusted with Ar/O2 mixture with no rerouting. This decision was made to simplify the experimental setup since the target is to just assess the viability of this concept. To avoid excessive argon consumption, the intake temperature was chosen to be at 25^{o}C to save the thermal equilibrium time. The running time was also optimized and all experiments were ran with CA50 at TDC and equivalence ratio 0.4. Testing conditions are summarized in Table 2.

Table 2: testing conditions

Parameter	**Value**
Speed	600 rpm
Tin	$25^oC \pm 2^oC$
Intake pressure	1 bar
CA50	TDC
Equivalence ratio ϕ (Fuel/oxygen)	≈ 0.4
Fuel	Isooctane

Exhaust emission analysis is crucial for this type of experiments not only to compare the emissions per se but also to evaluate the combustion efficiency which is the first step in the efficiency analysis. Fourier-transform infra-red (FTIR) emission analyzer was used for this purpose. The choice of the FTIR analyzer is because of simplicity and acceptable accuracy [27]. It can measure the emissions of main interest NOx, CO, and unburned

hydrocarbons (UHC). While it does not report total hydrocarbons as a conventional flame ionization detector (FID) would do, it still can report an approximate value based on individual measured species. Details about this technique could be found in appendix C.

2.2 Experimental setup

The experimental setup is built by connecting seven different systems that work together. Those are the engine itself which is a cooperative fuel research (CFR) engine, the fuel system, oxidizers mixing system, temperature control system, pressure measurement system, FTIR emission analyzer, and finally the computer system that synchronizes all these operations. The next subsections describe each system.

2.2.1 Cooperative fuel research (CFR) engine

The cooperative fuel research engine or simply CFR engine have been used in the 50's of last century for assessing the anti-knock quality of fuels [28]. It is a variable compression ratio engine that can relatively withstand and assess combustion abnormalities when compared to other engines. For this reason, it has been used for evaluating some novel concepts aiming for engine efficiency improvement. Figure 3 shows a picture of the CFR engine.

Figure 3: Cooperative fuel research (CFR) engine

The CFR engine shown in Figure 3 is the original engine and modifications have been made to this setup to meet our experimental requirements. The main modifications include replacing the intake by another one that enables better temperature control. Also, CFR

engine is designed to perform experiments in SI mode at near stoichiometric condition and a conventional carburetor is used for this purpose. But since it is intended to run the engine in HCCI lean conditions, the carburetor was replaced by a port fuel injector. Details about the fuel system will be demonstrated in the next section. One more modification made to the engine is replacing the nock detector by a pressure transducer to have a better monitoring of the combustion processes. Table 3 summarizes the specification of the CFR engine.

Table 3: characteristics of the Waukesha F1/F2 CFR engine

Parameter	Unit	Value
Displaced volume	cc	611.7
Stroke	mm	114.3
Bore	mm	82.55
Connecting rod	mm	256
Compression ratio	-	4:1 to 18:1
Number of valves	-	2
Exhaust valve opening	CA ATDC	140
Exhaust valve closure	CA ATDC	-345
Inlet valve opening	CA ATDC	-350
Inlet valve closure	CA ATDC	-146
Coolant water temperature	ºC	100 ± 1.5
Oil temperature	ºC	57 ± 8

2.2.2 Fuel system

As previously mentioned a port fuel injector was used to control the equivalence ratio. Fuel was pressurized by pressurized nitrogen and the amount of fuel injected was controlled by the injection timing. The flow rate was measured using a *Bronkhorst* liquid mass flow controller.

2.2.3 Oxidizer mixing system

Gases used for these experiments include air, nitrogen, oxygen, and argon. Thus, four different *Brooks* gas mass flow controller (MFC) were used to control the mixtures compositions. The partial pressure of each gas in an ideal gas mixture is equivalent to its

volume fraction. This is the concept used for mixing the gases. The flow rate of each gas adjusted was adjusted by the MFC in the required ratio to keep a total intake pressure of 1 bar. The intake pressure was measured by a pressure transducer mounted upstream near to the port fuel injector. This method was verified by comparing the results of the synthetic air mixture to the results obtained for the air mixture. The results chapter in this thesis will reveal that all results for these two mixtures were similar.

2.2.4 Temperature control system

Thermocouples are used to measure the intake, exhaust, and ambient temperatures. Exhaust and ambient temperatures are used to estimate the exhaust losses as will be shown in efficiency analysis. The intake temperature is regulated by two PID controlled electric heaters. The electric heaters were technically switched off since it was decided to conduct the experiments at an intake temperature of 25^{o}C to save the time of heating and thus reduce the amount of Argon wasted before the actual combustion starts.

2.2.5 Pressure measurement system

Three different pressure transducers were used. Two low pressure transducers for the intake and the exhaust and one transducer to measure the relatively higher in-cylinder pressure. All the transducers are piezoelectric sensors in which the mechanical stress generates a voltage difference. Pressure measurement system and signal processing are demonstrated in details in appendix A as they are an important component in the heat release analysis.

2.2.6 FTIR emission analyzer

An FTIR analyzer provided by *AVL* was used for measuring the exhaust emissions. The FTIR provides direct measurements for CO and NOx. The hydrocarbon based species can be added to estimate the total unburned hydrocarbons (UHC). Theory of operation and detailed experimental setup for this system can be found in appendix C.

Figure 4 demonstrates the experimental setup used in the experiments.

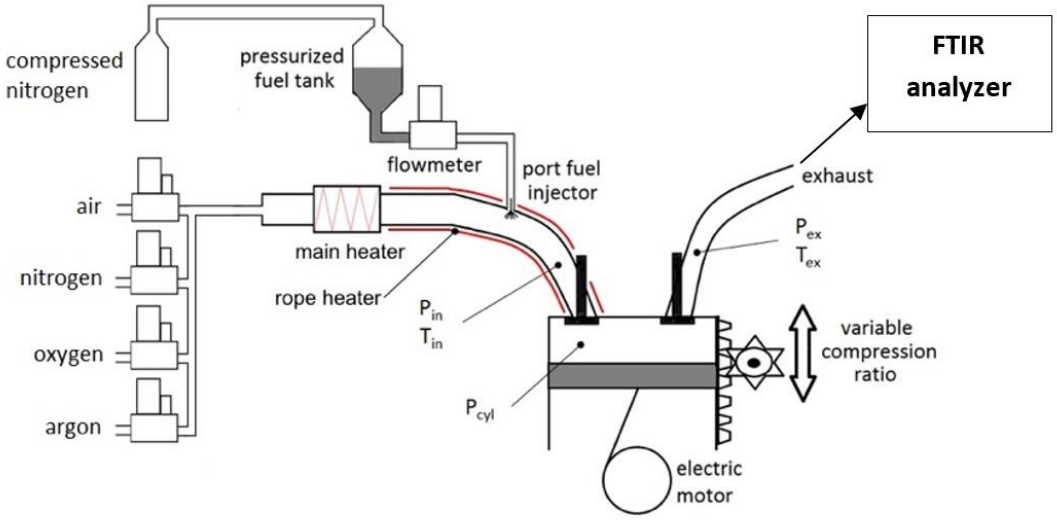

Figure 4: Schematic of the experimental setup

2.2.7 Computer system

Finally it is worth mentioning that the aforementioned systems were synchronized by an in-house developed LabVIEW program. The software enables the use to control all engine boundary conditions including engine speed, intake temperature, intake pressure, equivalence ratio, and volume compression ratio. MATLAB code was developed to analyze the results.

Chapter 3: Results and Discussions

Understanding the combustion behavior inside the engine is achieved by measuring the in-cylinder pressure. The in-cylinder pressure gives information about the physical properties of the gas. The most important physical property of the gas mixture in this research is the specific heat ratio. If isentropic relations are used as estimations for the gas compression (and also expansion), then the slope of the log-log P-V diagram will simply be the specific heat ratio since we know that $\frac{P_2}{P_1} = \left(\frac{V_1}{V_2}\right)^{\gamma}$ or $PV^{\gamma} = c$, Thus $\log P = \log c - \gamma \log V$, where c is a constant that can be determined. It is worth noting that this is just an estimation since the process is not ideally isentropic.

In-cylinder temperature can be inferred from the in-cylinder pressure using the ideal gas law. This is done because temperature is of special importance for HCCI mode where chemical properties are more important than the physical aspects of the cylinder.

Heat release analysis is of special importance since it reveals vital information about the rate of combustion and the energy released. Heat release analysis depends on pressure measurements that should be obtained accurately. Interested readers can consult appendix A for more information about the procedure of acquiring the pressure signal and the associated hear release analysis.

The battle for reducing exhaust emissions to protect the environment is still present. This chapter also highlights the emission results obtained and explains the abnormalities encountered. It is worth mentioning that exhaust emissions were measured using FTIR emission analyzer as previously highlighted in previous chapter. More information about the FTIR technique can be found in appendix C.

The chapter is concluded by the efficiency analysis results. The analysis focuses on the indicated thermal efficiency and it does not account for the mechanical efficiency of the engine. Actually, increasing the specific heat ratio is expected to increase the thermodynamic efficiency as preliminary calculations suggest. Combustion efficiency and gas exchange efficiency are also compared for different oxidizers. Finally, appendix B could be a suitable resource to understand the terminology associated with the efficiency analysis.

3.1 In-cylinder pressure

Figure 5 shows the measured in-cylinder pressure using the three different oxidizers.

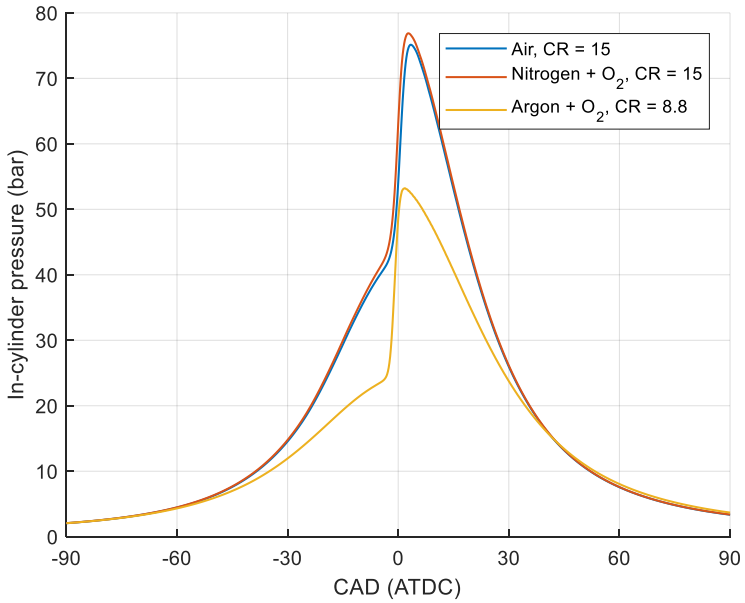

Figure 5: In-cylinder pressure traces with combustion phased with CA50 at TDC and equivalence ratio ϕ = 0.4

The combustion was phased to have CA50 at TDC. Thus the compression ratios for the mixtures are different. The CA50 at TDC was achieved at a compression ratio of 15 for both air and Oxygen/Nitrogen mixture while a compression ratio of 8.8 brought up the same combustion phasing with the Argon mixture.

A first thought could be that the argon mixture should have higher in-cylinder pressure because it has higher specific heat ratio. However, the preliminary calculations show that the in-cylinder pressure during the compression stroke is directly proportional to both the specific heat ratio as well as the compression ratio. It happens here that the effect of compression ratio outweighs the effect of increasing the specific heat ratio. Thus, the in-cylinder pressure is higher for air than for Argon. In fact, phasing the combustion to have similar CA50 for the three mixtures means that we are actually controlling the in-cylinder temperature and not the in-cylinder pressure as will be shown later.

As expected Air and Oxygen/Nitrogen mixtures had almost the same behavior. Actually, the primary purpose for running the engine with Oxygen/Nitrogen mixture was to make sure that the previously mentioned partial pressures mixing of the gases is properly working and giving reliable results.

3.2 P-V diagrams

P-V diagrams are indicators of the work produced on the piston and also the pumping losses during gas exchange. Figure 6 shows the P-V diagrams obtained from the three different mixtures.

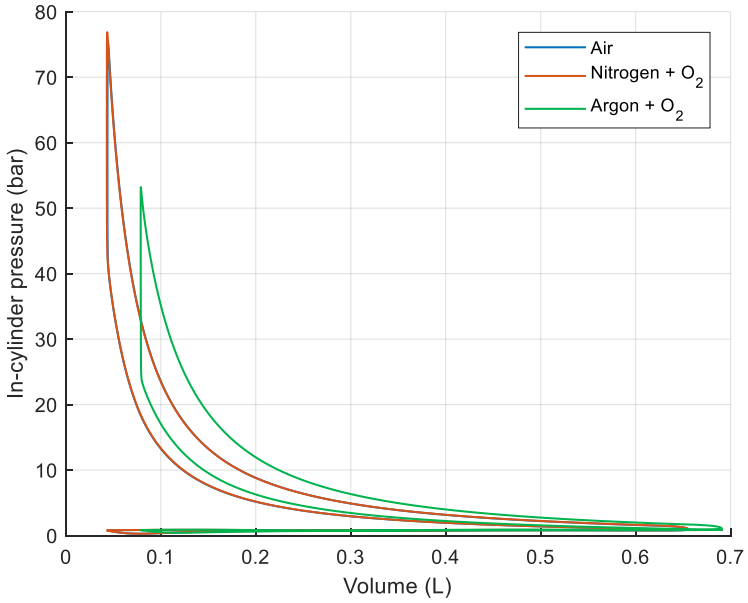

Figure 6: P-V diagrams for the three cases. The air and N_2/O_2 mixtures are overlapping.

One can easily see that the compression ratios are different. One important observation here is that heat is added at almost constant volume at TDC. This behavior is expected since in HCCI almost all the charge is excited at the same time and heat is released way faster than a conventional spark ignited engine or even a compression ignition spray controlled combustion.

Figure 7 and Figure 8 show gas exchange zoomed version of Figure 6.

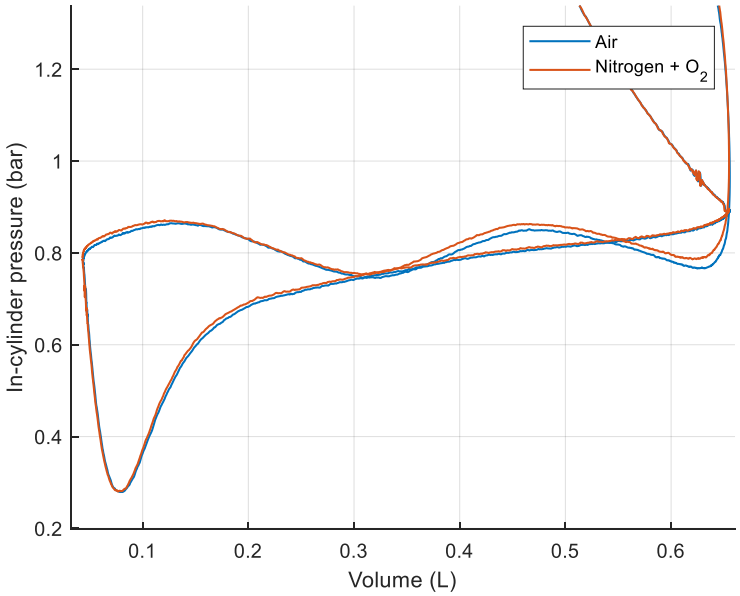

Figure 7: P-V diagram gas exchange zoom-in for air and N_2/O_2 mixtures

The enclosed area during gas exchange represents the pumping losses and we expect that the Argon mixture will have higher pumping losses because it is heavier than other mixtures. Argon in fact has a molar mass of approximately 40 kg/kmol while air and Oxygen/Nitrogen mixtures have a molar mass of around 29 kg/kmol. The gas exchange for argon mixture is shown in Figure 8.

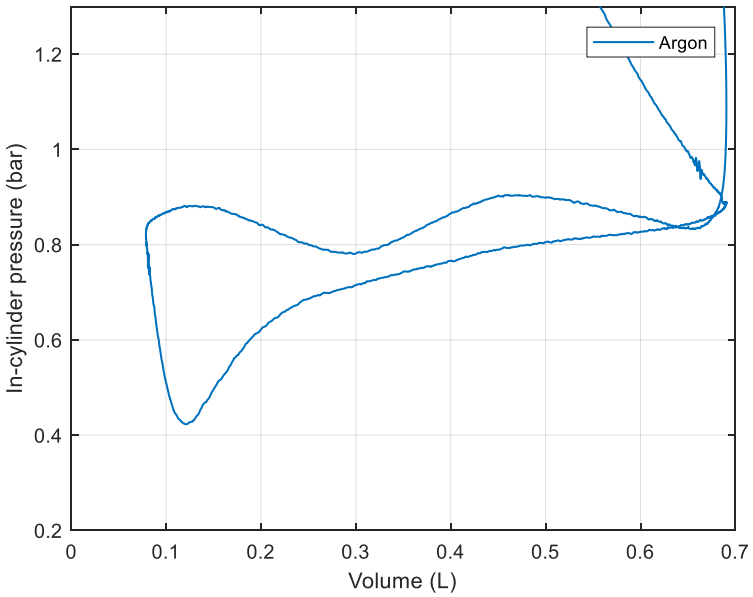

Figure 8: P-V diagram gas exchange zoom-in for the argon mixture

It is difficult to notice the pumping losses differences by observing figures Figure 7 and Figure 8. However, later in this paper the efficiency analysis will reveal that the pumping losses for the Argon mixture are higher as expected.

Finally, one more interesting result is observed if the log-log P-V diagram is plotted since the slope of the compression and expansion strokes will be close to the specific heat ratio if isentropic relations are assumed. Figure 9 shows a log p-log V diagram and the obtained slopes.

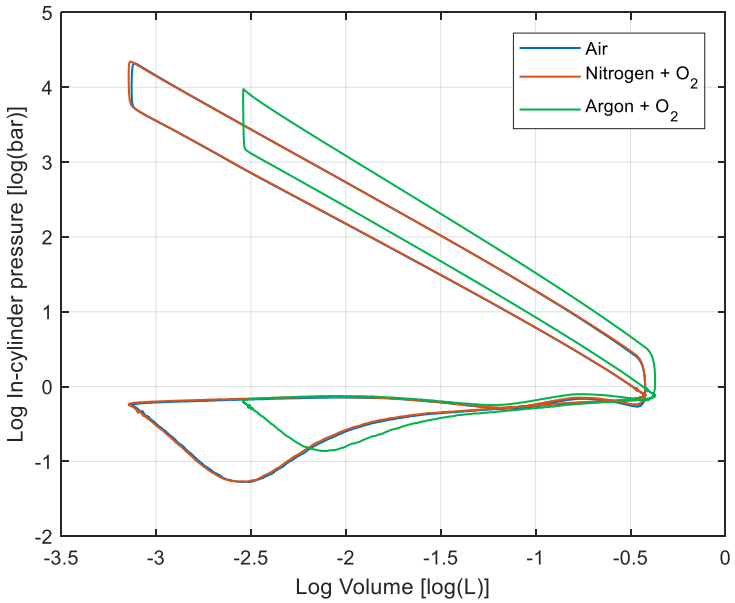

Figure 9: log P-log V diagrams for the three cases. The air and N2/O2 mixtures are overlapping.

As expected the plot shows that the slope of the argon mixture is higher meaning that the specific heat ratio is increased by using Argon in the mixture.

3.3 In-cylinder Temperature

In-cylinder temperature plays a vital role in HCCI engines. The temperature has to be high enough for the charge to autoignite and also to oxidize CO to CO2; nonetheless, temperature should not be significantly high to prevent the formation of NOx. Figure 10 shows the in-cylinder temperature obtained from the pressure traces using the ideal gas law.

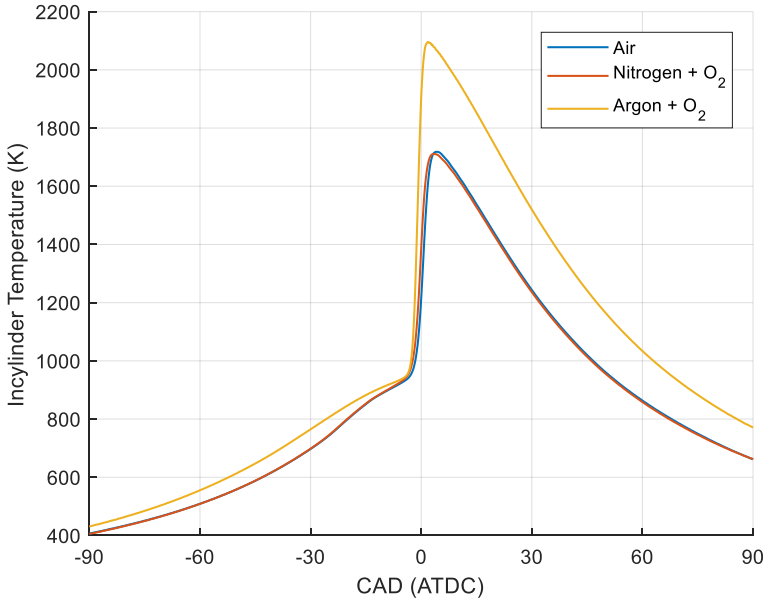

Figure 10: In-cylinder temperature traces with combustion phased with CA50 at TDC and equivalence ratio φ = 0.4

It is a role of thump that autoignition in HCCI engine will be activated at an in-cylinder temperature close to 1000 K. Figure 10 demonstrates this behavior where the combustion for all gas mixtures starts at almost 950 K. It is worth noting here that it was intended to have the same combustion phasing for all gas mixtures and it can be noticed that combustion starts at the same CAD.

The temperature increase of Air and Oxygen/Nitrogen mixtures is almost 2/3 of the Argon mixture. This is because of the specific heat difference of the two mixtures. Starting from $\Delta T = Q/mc_p$ one can find the following relation

$$\frac{\Delta T_{air}}{\Delta T_{Ar+O_2}} = \left(\frac{Q_{air}}{Q_{Ar+O_2}}\right)\left(\frac{m_{Ar+O_2}}{m_{air}}\right)\left(\frac{c_{p,Ar+O_2}}{c_{p,air}}\right) \quad (2)$$

Where

ΔT: the temperature increase
Q: the heat added by burning the fuel
m: the total mass including the mass of the oxidizer mixture and fuel
c_p: the specific heat of the gas
the subscripts denote air (also Oxygen/Nitrogen mixture since they are almost the same) and the argon mixture respectively.

In equation 2, $\left(\frac{Q_{air}}{Q_{Ar+O_2}}\right) \approx 1$ since equivalence ratio is the same. Also, the molar mass of Argon is approximately 40 kg/kmol while it is almost 30 kg/kmol for air giving $\left(\frac{m_{Ar+O_2}}{m_{air}}\right) \approx \frac{4}{3}$ and finally $\left(\frac{c_{p,Ar+O_2}}{c_{p,air}}\right) \approx \frac{1}{2}$ giving $\frac{\Delta T_{air}}{\Delta T_{Ar+O_2}} \approx \frac{2}{3}$ which is approximately the experimental result. However, this justification is approximate since injected energy is not quite the same. Fixing the equivalence ratio does not mean having the same mass of fuel injected. This is highlighted later in this paper when discussing the heat release rates. Also, Argon is mixed with oxygen and this will decrease the effective molecular weight but since argon is the major constituent, the approximation is acceptable.

It is common practice in engine research to assume that the exhaust losses could be approximated by the enthalpy change of the exhaust gases. While the temperature of the argon mixture exhaust is higher it still has less specific heat ratio. This means that it is expected to have almost the same exhaust losses independent of the working media. This result is highlighted more in the efficiency analysis section later in this paper.

3.4 Heat release rate (HRR)

Ideal gas law can be used to estimate the heat release rate inside the engine cylinder as per the following equation:

$$\frac{dQ_{hr}}{d\theta} = \frac{\gamma}{\gamma - 1} p \frac{dV}{d\theta} + \frac{1}{\gamma - 1} V \frac{dp}{d\theta} + \frac{dQ_{ht}}{d\theta} \quad (3)$$

Where

$\frac{dQ_{hr}}{d\theta}$: the heat release rate (HRR) per crank angle degree (CAD)
γ : the specific heat ratio $\frac{c_p}{c_V}$
p : the in-cylinder pressure
V : the volume of the cylinder
$\frac{dV}{d\theta}$: the rate of volume change per crank angle degree
$\frac{dp}{d\theta}$: the rate of pressure change per crank angle degree
$\frac{dQ_{ht}}{d\theta}$: the rate of heat transfer losses per crank angle degree

In this analysis crevice and blow-by losses were neglected. The model only considers heat transfer losses that represent the major losses. Woschni [9] developed a model to estimate the heat transfer losses. To the authors' knowledge, Wochni heat transfer model is the most popular model among researchers in internal combustion engines community.

Although the model is simple, it is able to estimate heat losses with an acceptable accuracy. Simplicity here means that it predicts heat losses from the in-cylinder pressure that is relatively easy to measure.

Equation 3 shows that heat release rate depends on the specific heat ratio γ. Specific heat ratio is not a constant a physical property and it depends on the temperature. For this reason, a two zone model was developed to accurately model the specific heat ratio for the mixtures. Those two zones are the reactants and the products assuming complete combustion. The mixture is assumed to have either reactants before TDC or products after TDC. Nasa polynomials along with coefficients taken from Burcat's tables [29] were used to estimate the specific heats of the working fluids. Figure 11 shows the results of this model.

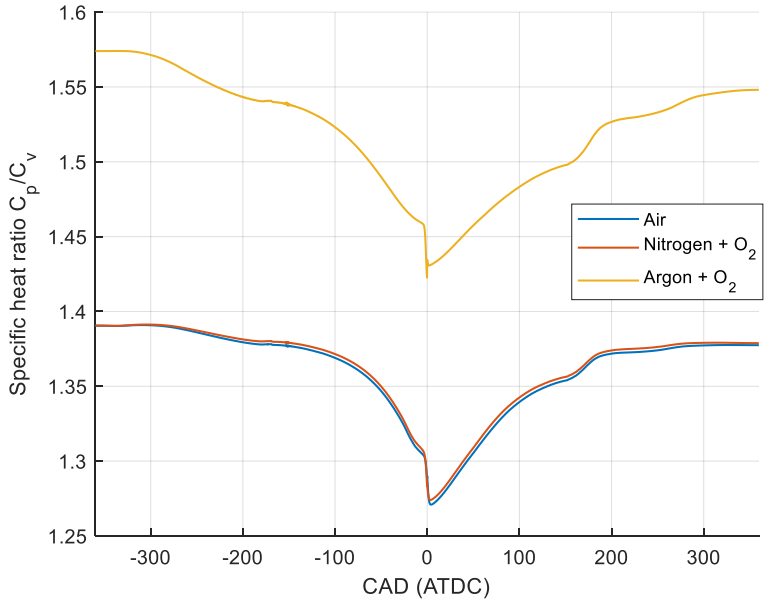

Figure 11: model results for the specific heat ratio as a function of CAD. The variation is due to the temperature change and combustion reactions.

It can be noticed that the specific heat ratio is disturbed at the time of exhaust valve opening (EVO). This is because of the sudden disruption of the in-cylinder temperature. The results of the model show that it is sufficient to have a two zone model since, for both reactants and products, there is a sharp decrease in specific heat ratio at TDC. Thus, it can be assumed that they are almost the same and there will be no much difference if intermediate species are also included. Of course, a highly accurate model could be developed by using a more sophisticated chemical kinetics model.

It is worth noting here that the sharp decrease in specific heat ratio at TDC is because of the high in-cylinder temperature that enables the gas molecules to obtain more degrees

of freedom and hence have lower specific heat ratio. One more interesting observation is that the Argon mixture does not have a specific heat ratio as high as 1.67 which is the theoretical specific heat ratio for argon. The reason is that argon is not the only constituent but it is mixed with oxygen and isooctane that have much lower specific heat ratios. Finally, it is clear that the argon mixture have higher specific heat ratio than Air and Oxygen/Nitrogen mixtures as expected even at higher temperatures close to TDC.

Figure 12 shows the Heat release rates obtained for the three different mixtures.

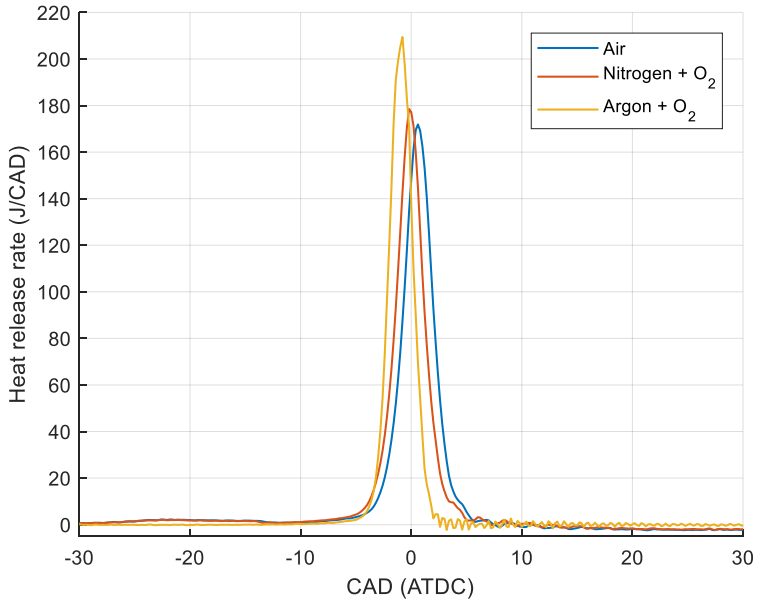

Figure 12: Heat release rates for the three different mixtures

The heat release rate is faster in the case of the argon mixture. This is a direct result of the elevated temperature shown in Figure 10. As previously mentioned, temperature is the main driver of the combustion kinetics in HCCI combustion mode and most of heat release phenomena are linked to temperature. It is expected that the air and nitrogen/oxygen mixture should have the same heat release rate and this is almost what the experiment is showing. However, there is still a small difference attributed mainly to the composition difference and the experimental variations.

One more interesting result is that in the case of air and nitrogen/oxygen mixture low temperature reactions are observed while the argon mixture seems to suppress this low temperature heat release (LTHR). Those reactions are expected since we have a low intake temperature even when we are using a high octane fuel (Cite Waqas). Argon on the other hand seems to suppress the fuel reactivity. This result is interesting for further

investigation since results in rapid compression machine (RCM) have shown no significant difference on the fuel reactivity between argon and nitrogen [30], [31].

While argon mixture has faster combustion rate, the accumulated heat released is still lower than air and nitrogen/oxygen mixture. Figure 13 highlights that result. It can be easily noticed that CA50 is at TDC and the heat starts to be released 10 CAD BTDC.

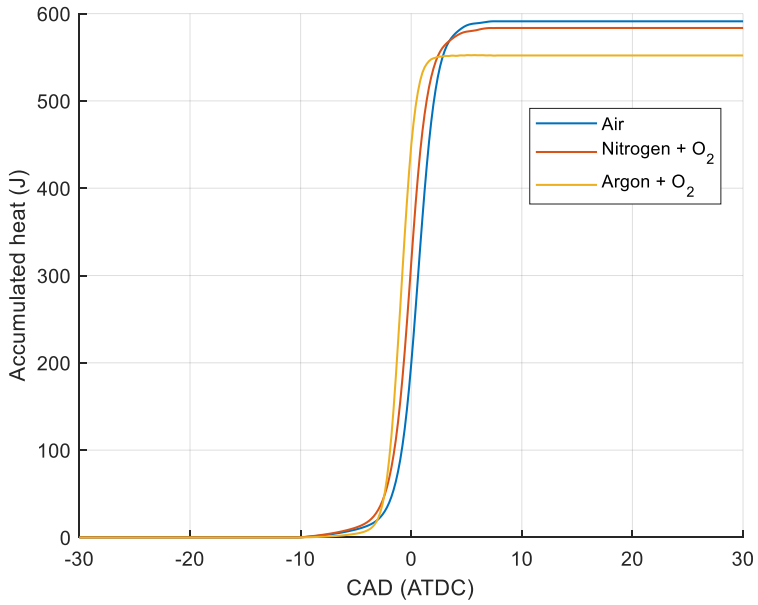

Figure 13: Accumulated heat release for the three different mixtures

Results shown in Figure 13 are interesting since they suggest that accumulated heat released are less for argon. If the temperature is higher in the case of argon mixture then the reasonable result is that argon mixture will have higher accumulated heat released. However, Figure 13 is energy based and it depends on the mass of fuel injected to the cylinder. Fixing the equivalence ratio at 0.4 resulted in less fuel injected for the argon mixture.

3.5 Efficiency analysis

This analysis focuses on the indicated thermal efficiency that is the overall all engine efficiency excluding the engine mechanical efficiency. Interested reader can find more information about the calculations and procedures followed to evaluate those efficiencies in appendix B.

3.5.1 Combustion efficiency

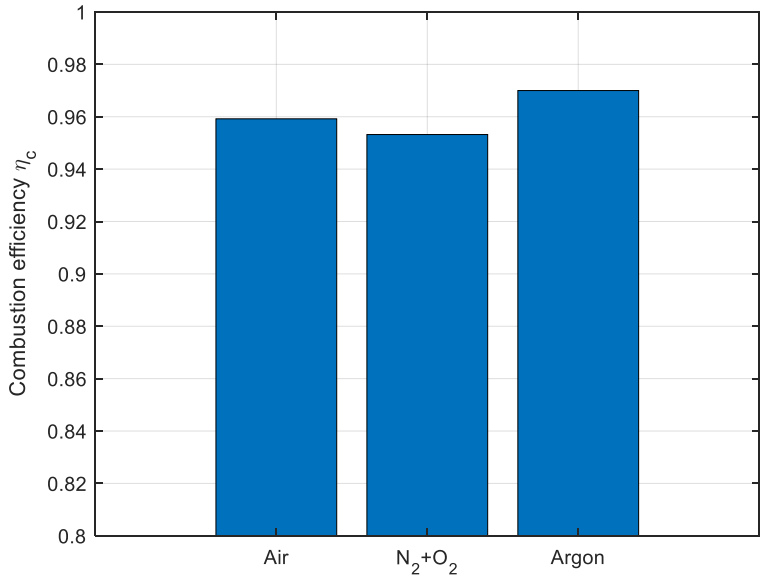

Figure 14: Combustion efficiency for the three different mixtures

The combustion efficiency was almost the same for all three cases as shown in Figure 14. As expected argon mixture has slightly higher combustion efficiency due to the increased in cylinder temperature that assists the oxidation of the isooctane. This result can also be observed from the exhaust analysis where hydrocarbon concentration was minimum in the case of argon mixture.

3.5.2 Thermodynamic efficiency

Thermodynamic efficiency is the main result of this research. As previously discussed increasing the specific heat ratio is expected to increase the engine thermodynamic efficiency. The results obtained suggest that argon increase the engine thermodynamic efficiency but at the same time the increment was limited. Actually, argon mixture increased the efficiency approximately 5% from the results obtained for the air mixture. Figure 15 shows the thermodynamic efficiency for the three different mixtures.

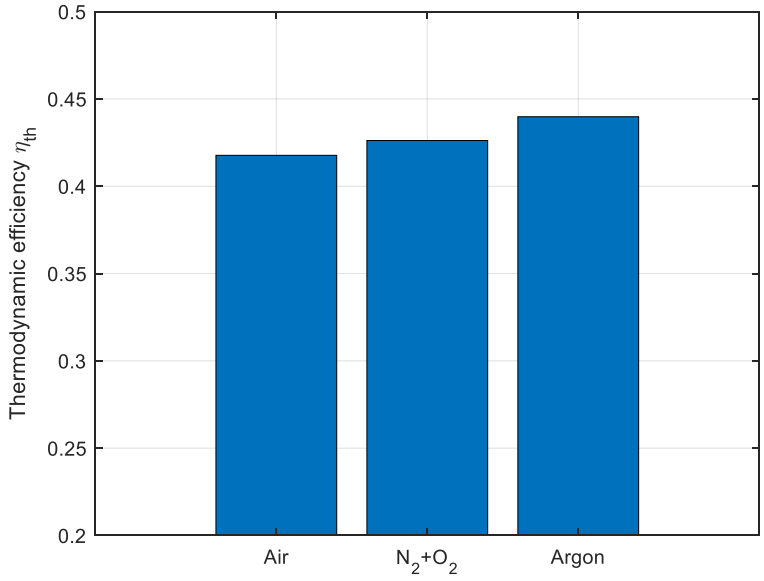

Figure 15: Thermodynamic efficiency for the three different mixtures

The combustion was phased to have a CA50 at TDC and this fixed the compression ratios to 15 for the air and nitrogen/argon mixtures and 8.8 for the argon mixtures. One can estimate the theoretical thermodynamic efficiency using these two compression ratios along with assumed specific heat ratios (1.35 for air and 1.67 for argon).

Table 4: Comparison between the theoretical and actual thermodynamic efficiency

Oxidizers	$\eta_{th,theoritical}$	$\eta_{th,experimental}$	$\frac{\eta_{experimental}}{\eta_{theoritical}}$
Air	50%	42%	84%
$N_2 + O_2$	62%	42.5%	68.5%
$Ar + O_2$	68%	44%	65%

Table 4 shows that although the argon mixture increased the thermodynamic efficiency of the engine it reduced its ability to attain the maximum theoretical efficiency. This is due to the increased heat transfer losses as a result of relatively higher in-cylinder temperature. Figure 16 shows a comparison between experimentally obtained thermodynamic efficiency and the ideal thermodynamic efficiency assuming specific heat ratio at TDC temperature. One can easily notice that the argon mixture cannot has lower ideal thermodynamic efficiency than pure argon. The reason is that argon mixture contains not only argon but also oxygen and fuel that significantly decrease the effective specific heat ratio.

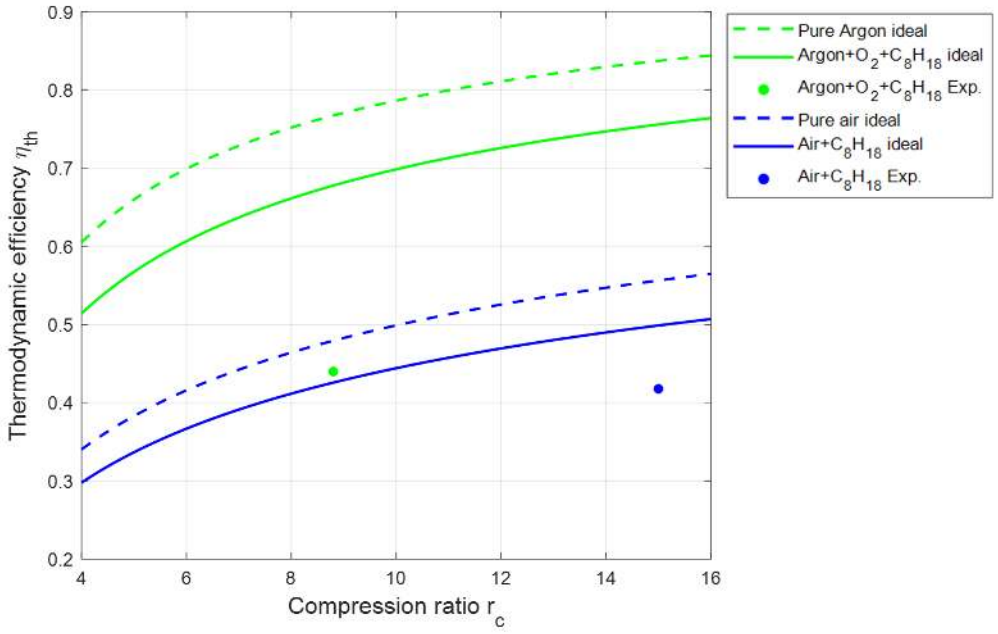

Figure 16: Comparison between ideal thermodynamic efficiency with specific heat ratio at TDC and experimentally obtained thermodynamic efficiency

3.5.3 Gas exchange efficiency

Part of the mechanical work exerted on the piston is used to pump the exhaust out of the engine. The consumed energy in this process reduces the engine efficiency. Gas exchange efficiency is used to evaluate this process. Figure 17 shows that the argon mixture has the lowest gas exchange efficiency and this is a direct result of the higher argon density that requires more pumping work as highlighted before when discussing the P-V diagrams. However, there are still no considerable differences between the three cases.

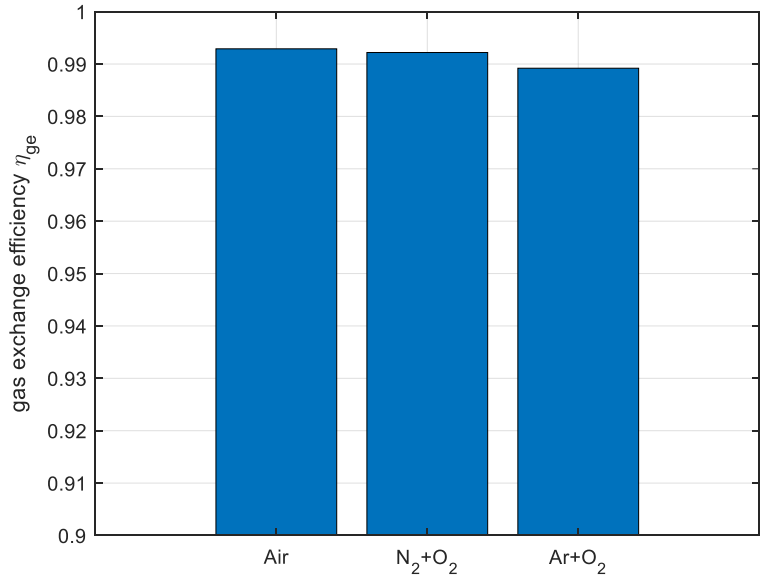

Figure 17: Gas exchange efficiency for the three different mixtures

3.5.4 Indicated thermal efficiency

Indicated thermal efficiency $\eta_{ind,th}$ is the lumped efficiency excluding the mechanical efficiency. Thus,

$$\eta_{ind,th} = \eta_c \, \eta_{th} \, \eta_{ge} \tag{4}$$

Figure 18 shows that the indicated thermal efficiency was the highest for the argon mixture as expected.

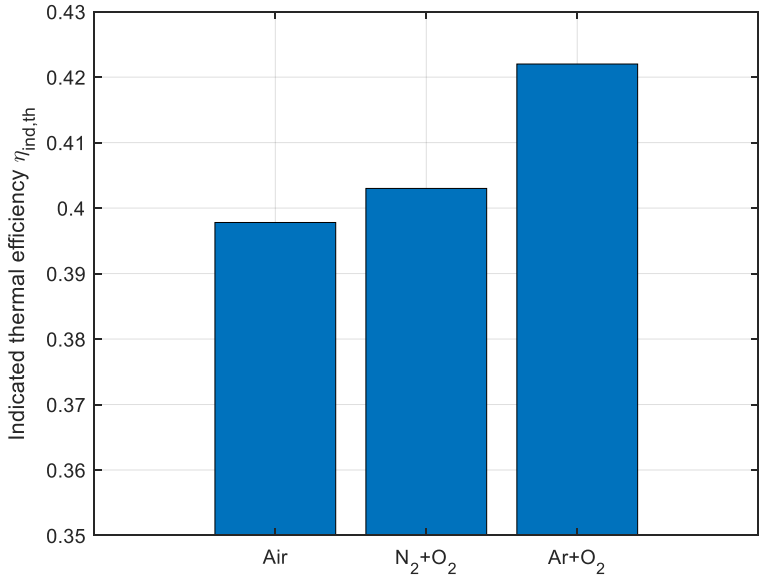

Figure 18: Indicated thermal efficiency for the three different mixtures

Finally, figure 19 summarizes these efficiency results. One can easily observe that the use of argon increased all efficiencies except the gas exchange efficiency due to its higher density.

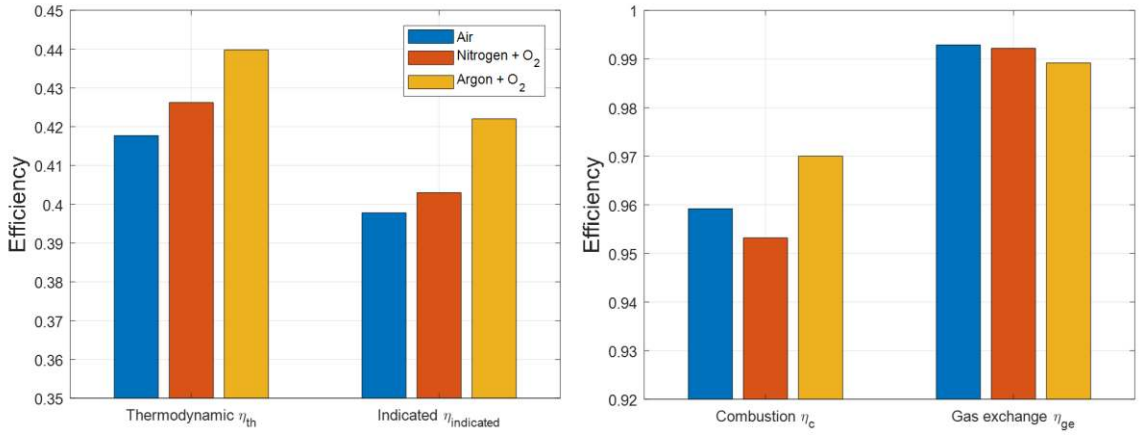

Figure 19: Efficiency results for the three different mixtures

3.6 Exhaust emissions

The high in-cylinder temperature in the case of argon mixture explains many phenomena observed and the concentration of the hydrocarbons and carbon monoxide in the exhaust is no exception.

As expected the high temperature in the case of the argon mixture resulted in less hydrocarbon concentration, almost 40% less than the air and nitrogen/oxygen mixtures.

The same trend is observed for the carbon monoxide in which the elevated temperature assists the oxidation of CO into CO_2. Figure 20 and figure 21 show the concentration of UHC and CO acquired from the FTIR emission analyzer respectively.

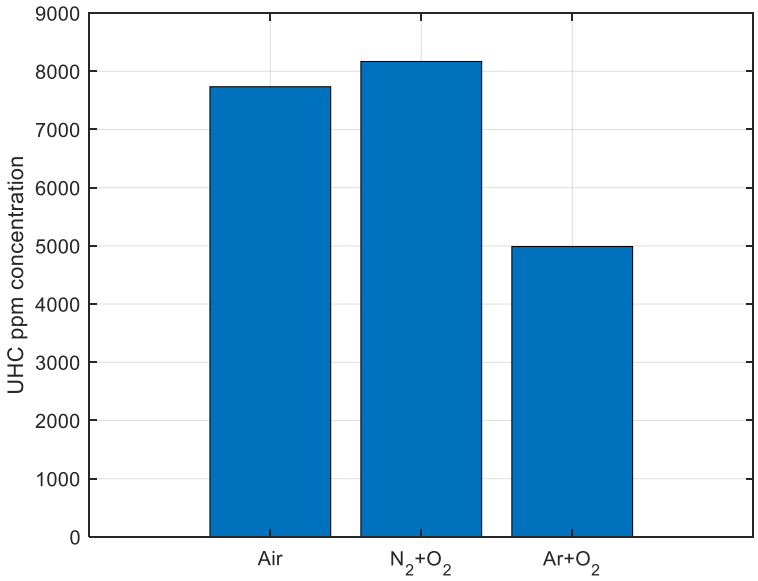

Figure 20: Unburned hydrocarbons emission results.

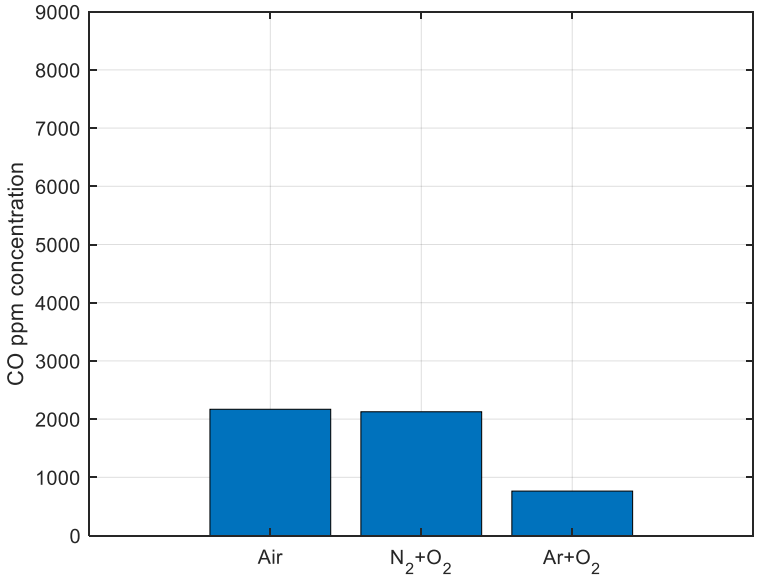

Figure 21: Carbon monoxide emission results

Nitrogen oxides (NOx) formation is described by a mechanism known as the Zeldovich extended mechanism introduced by Lavoie et al. [32]. The formation of NOx is a strong function of temperature in which higher temperature means higher NOx concentration. For this reason it is customary to call the NOx formed by this mechanism as thermal NOx.

Figure 22 shows the NOx measurements obtained for the three different mixtures. The measured NOx concentration is very low and (note the difference in scale between figure 22 and figures 20-21). This is expected since HCCI is a low temperature combustion technique. However, the result for the argon mixture is confusing since no nitrogen was supplied to the engine and yet there are still nitrogen oxides in the exhaust. The experiment has been repeated three times to investigate whether this was just an experimental error but the same results were obtained every time. It was then realized that small nitrogen traces in the oxygen and argon cylinder were oxidized at the argon elevated temperature. In fact, the cylinders used in the experiment are contaminated with 15 ppm of Nitrogen and almost all the N_2 atoms have been oxidized due to the in-cylinder high temperature justifying the obtained result.

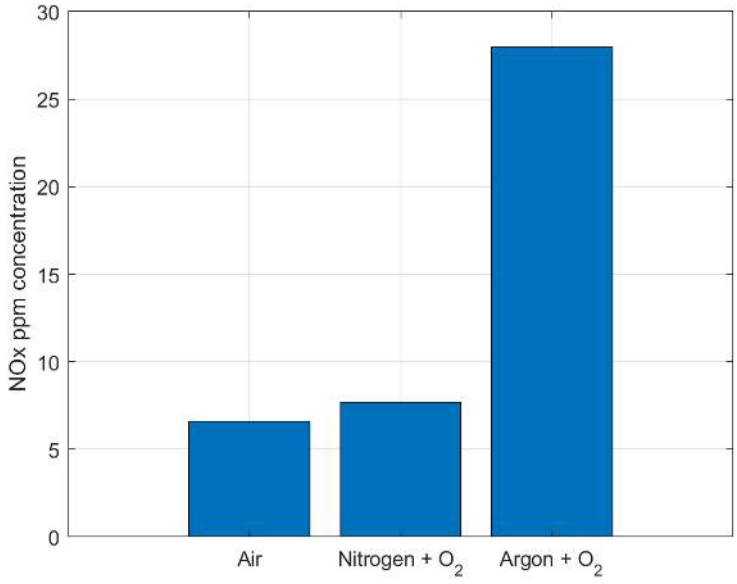

Figure 22: NOx emission results

The next chapter summarizes the main conclusions withdrawn from these experimental results.

Chapter 4: Conclusions

The present study investigated the potential of argon, a gas with high specific heats ratio, for replacing nitrogen contained into the air in order to reach high-efficiency engine. Experiments were performed under HCCI conditions with isooctane as fuel using a modified single cylinder variable compression ratio CFR engine. Three different oxidizers mixtures were considered: compressed air, synthetic air and argon + oxygen. All the experiments were conducted with fixed conditions and only the compression ratio has been adjusted to keep a constant combustion phasing. In-cylinder pressures and resulting relevant engine outputs as well as emissions were analyzed and compared. The following conclusions were drawn:

- Argon replacing nitrogen required a lower compression ratio in order to maintain a fixed combustion phasing. The resulting pressure trace is therefore lower for the case with argon but the pressure rise rate remains aggressive.
- Temperature traces were found higher with argon but the autoignition occurs at a similar crank angle and when mixtures reached the critical temperature of 950 K. Argon and nitrogen are therefore non-dependent species for the autoignition of isooctane.
- Heat release rates showed that argon led to shorter combustion duration and more aggressive combustion. Nonetheless, the energy inducted into the cylinder is less such as argon might help in reducing fuel consumption.
- Argon increased thermal efficiency by approximately 6%.
- HC and CO emissions are significantly reduced because of the less amount of fuel injected and because of the higher in-cylinder temperatures reached.
- Higher NOx emissions with argon were detected but those results were attributed to the experimental setup which might have allowed some nitrogen to be injected during the argon cycle.

The present study emphasized the potential of argon. Nonetheless, further investigations by comparing with other gases should be performed. Moreover, other fuel like hydrogen might replace isooctane in future results such as a high-efficiency zero-emissions combustion cycle should be proposed.

BIBLIOGRAPHY

[1] R. Lee, “The Outlook for Population Growth,” vol. 333, no. July, pp. 569–574, 2011.

[2] “World Energy Outlook 2017,” 2017.

[3] U. S. Energy, “International Energy Outlook 2017 Overview,” 2017.

[4] J. I. M. De Groot and L. Steg, “Morality and Nuclear Energy : Perceptions of Risks and Benefits , Personal Norms , and Willingness to Take Action Related to Nuclear Energy,” vol. 30, no. 9, 2010.

[5] L. Huang, Y. Zhou, Y. Han, J. K. Hammitt, J. Bi, and Y. Liu, “Effect of the Fukushima nuclear accident on the risk perception of residents near a nuclear power plant in China,” vol. 110, no. 49, pp. 19742–19747, 2013.

[6] “GLOBAL TRENDS IN RENEWABLE ENERGY INVESTMENT 2018,” 2018.

[7] J. P. Hansen, P. A. Narbel, and D. L. Aksnes, “Limits to growth in the renewable energy sector,” *Renew. Sustain. Energy Rev.*, vol. 70, no. March 2016, pp. 769–774, 2017.

[8] G. Kalghatgi, “Is it really the end of internal combustion engines and petroleum in transport ?,” *Appl. Energy*, vol. 225, no. February, pp. 965–974, 2018.

[9] G. Woschni, “A Universally Applicable Equation for the Instantaneous Heat Transfer Coefficient in the Internal Combustion Engine,” in *National Fuels and Lubricants, Powerplants, Transportation Meetings*, 1967.

[10] N. Lam, M. Tuner, P. Tunestal, A. Andersson, S. Lundgren, and B. Johansson, “Double Compression Expansion Engine Concepts : A Path to High Efficiency,” pp. 1562–1578, 2018.

[11] H. A. Moneib, M. Abdelaal, M. Y. E. Selim, and O. A. Abdallah, “Effects of Diluting the Intake Air of SI Engine with Argon Inert Gas on the NOx Emissions and Performance,” in *SAE World Congress & Exhibition*, 2009.

[12] W. Li, Z. Liu, Z. Wang, C. Li, L. Duan, and H. Zuo, “Effect of CO2, N2, and Ar on Combustion and Exhaust Emissions Performance in a Stoichiometric Natural Gas Engine,” *SAE Int. 2014-01-2693*, vol. 2, 2014.

[13] E. Eckermann, *World History of the Automobile*. Society of Automotive Engineers, 2001.

[14] P. C. T. De Boer, W. J. McLean, and H. S. Homan, “Performance and emissions of hydrogen fueled internal combustion engines,” *Int. J. Hydrogen Energy*, vol. 1, no. 2, pp. 153–172, 1976.

[15] S. Furuhama, M. Hiruma, and Y. Enomoto, “Development of a liquid hydrogen car,” *Int. J. Hydrogen Energy*, vol. 3, no. 1, pp. 61–81, 1978.

[16] Z. J. Wu, X. Yu, L. Z. Fu, J. Deng, Z. J. Hu, and L. G. Li, “A high efficiency oxyfuel internal combustion engine cycle with water direct injection for waste heat recovery,” *Energy*, vol. 70, pp. 110–120, 2014.

[17] Z. Kang, Z. Wu, Z. Zhang, J. Deng, Z. Hu, and L. Li, “Study of the Combustion Characteristics of a HCCI Engine Coupled with Oxy-Fuel Combustion Mode,” *SAE Int. J. Engines*, vol. 10, no. 3, pp. 2017-01–0649, 2017.

[18] H. Li and G. A. Karim, “The Performance of a Hydrogen-Oxygen SI engine,” vol. 2002, no. 724, 2002.

[19] A. Boretti, A. Osman, and I. Aris, “Direct injection of hydrogen, oxygen and water in a novel two stroke engine,” *Int. J. Hydrogen Energy*, vol. 36, no. 16, pp. 10100–10106, 2011.

[20] E. Lauman and R. Reynolds, “Hydrogen-Fueled Engine,” 1976.

[21] P. C. T. de Boer and J.-F. Hulet, “Performance of a hydrogen-oxygen-noble gas engine,” *Int. J. Hydrogen Energy*, vol. 5, no. 4, pp. 439–452, 1980.

[22] R. Kuroki, A. Kato, E. Kamiyama, and D. Sawada, “Study of High Efficiency Zero-Emission Argon Circulated Hydrogen Engine,” 2010.

[23] N. J. Killingsworth, V. H. Rapp, D. L. Flowers, S. M. Aceves, J. Y. Chen, and R. Dibble, “Increased efficiency in SI engine with air replaced by oxygen in argon mixture,” *Proc. Combust. Inst.*, vol. 33, no. 2, pp. 3141–3149, 2011.

[24] M. S. Aznar *et al.*, “Experimental investigation of port and direct injection strategies for internal combustion engines with argon as the working fluid,” *Proc. Eur. Combust. Meet. 2017*, no. April, pp. 1–6, 2017.

[25] N. M. Hafiz, M. R. A. Mansor, W. M. F. Wan Mahmood, and M. Shioji, “Simulation of the Effect of Initial Temperature and Fuel Injection Pressure on Hydrogen Combustion Characteristics in Argon-Oxygen Compression Ignition Engine,” 2016.

[26] R. W. Dibble, “Recirculating Noble Gas Internal Combustion Power Cycle,” 2017.

[27] B. Daham *et al.*, “Application of a Portable FTIR for Measuring On-road Emissions,” in *SAE 2005 World Congress & Exhibition*, 2005.

[28] ASTM, “Standard Test Method for Motor Octane Number of Spark-Ignition Engine Fuel 1,” *Annu. B. ASTM Stand.*, no. C, pp. 1–56, 2011.

[29] A. Burcat, “Third Millennium Ideal Gas and Condensed Phase Thermochemical Database for Combustion with Updates from Active Thermochemical Tables,” no. September, 2005.

[30] H. Di *et al.*, “Effects of buffer gas composition on low temperature ignition of iso-octane and n-heptane,” *Combust. Flame*, vol. 161, no. 10, pp. 2531–2538, 2014.

[31] S. W. Wagnon and M. S. Wooldridge, “On the effects of diluent gas composition on autoignition,” *8th US Natl. Combust. Meet. 2013*, vol. 2, no. 4, pp. 898–907, 2013.

[32] G. A. Lavole, J. B. Heywood, and J. C. Keck, “Experimental and theoretical study of nitric oxide formation in internal combustion engines,” *Combust. Sci. Technol.*, vol. 1, no. 4, pp. 313–326, 1970.

[33] E. Singh, M. Waqas, B. Johansson, and M. Sarathy, “Simulating HCCI Blending Octane Number of Primary Reference Fuel with Ethanol,” no. Ci, 2017.

[34] B. Johansson and L. universitet. Institutionen för energivetenskaper, *Combustion Engines*, no. v. 1. Department of Energy Sciences, Lund University, 2014.

[35] D. M. Himmelblau, *Basic Principles and Calculations in Chemical Engineering*, no. v. 1. Prentice Hall PTR, 1996.

[36] T. C. C. De Melo *et al.*, “Hydrous ethanol-gasoline blends - Combustion and emission investigations on a Flex-Fuel engine,” *Fuel*, vol. 97, pp. 796–804, 2012.

APPENDICES

Appendix A: Heat release analysis

A.1 Introduction

Heat release analysis is used to study and understand the combustion behavior inside the engine. It gives information about rate of combustion and can also be used to understand the fuel behavior and the tendency to knock [33]. In this chapter we will discuss how heat release could be obtained from an engine. The major step is to measure the in-cylinder pressure and then refine the obtained signal. Thermodynamic relations are then used to obtain a formula for heat release rate inside the engine using in-cylinder pressure and volume. Many models to estimate the heat losses were developed and those are discussed concisely. One important heat loss model is then explained and used in this analysis that is the Woschni heat loss model. Finally, we discuss the tuning of the heat release model.

A.2 Pressure measurement

The easiest physical quantity that can be measured inside a combustion engine is pressure. In-cylinder temperature cannot be measured easily because no thermocouples can sustain the usually high in-cylinder temperatures. Instead, the measured pressure is used to find the in-cylinder temperature. There are three main equipment used in measuring the in-cylinder pressure. Those are the pressure transducer, the amplifier, and the A/D converter.

A.2.1 Signal generation

The most common equipment to measure the in-cylinder pressure among engine researchers is the piezoelectric pressure transducer. It is based on the piezoelectric effect in which a charge is generated when a mechanical stress is applied on that piezoelectric material. The reason for that is the shifting of positive and negative charge centers of this specific type of material upon the application of a mechanical stress. The piezoelectric effect is also reversible meaning that the application of an electrical field also generates produces either compression or stretching of the material.

The piezoelectric pressure transducer consists of a piezoelectric crystal that is mounted in the cylinder head. Positioning of the pressure transducer plays an important role since in many cases it will not capture the in-cylinder pressure oscillations that detect knock. The in-cylinder pressure applies a mechanical stress on the piezoelectric material and hence a charge is generated in the crystal. This generated charge is connected by a special cable to a charge amplifier that generate a voltage proportional to the generated charge and of course the mechanical stress generated by the in-cylinder pressure. A special cable here means that it should be highly resistive (in the order of 10^{13} Ω). The reason is that very small currents flow in that wire and there is a high possibility that nearby electrical fields will interfere and bring noise to the measured signal. This also means that this cable should be as short as possible to prevent any background interference.

The generated voltage by the charge amplifier is actually an analog signal that represents the physical phenomena. This analog signal should then be digitized by a special device called the analog/digital converter shortly the A/D converter to be able to process the signal using a computer. The A/D converter involves a series of processes including sampling, quantization and coding. The details of the signal processing happening in the A/D converter is out of the scope of this thesis.

It is worth noting here that the pressure measurements are obtained as a function of crank angle degree by using a device called crank encoder that enables reporting the in-cylinder pressure at a specific CAD. Every encoder has its own resolution. The encoder used in this research during had a resolution of 0.2 CAD meaning that it can register a measurement at each 0.2 CAD.

Finally, it should be noted that the intake and exhaust pressures measurements are also needed for controlling the intake pressure and for further efficiency analysis. The next appendix about the efficiency analysis will reveal that exhaust and intake pressures could be used to estimate the pumping losses with a fairly acceptable accuracy.

A.2.2 Pegging of the pressure signal

The A/D converter reports the pressure signal in terms of A/D converter counts. However, a researcher will be interested in having the pressure in terms of pressure units like bar, kPa, psi, … etc. The process in which the A/D converter counts are transformed to pressure units is simply called pegging of the in-cylinder pressure. Specifically and in more scientific terms, the close to zero signal due to the charge leakage in the amplifier causes the signal level to depend on the pressure during the compression and expansion strokes. Thus, an absolute value should be fixed (and hence the name pegging) and other data should be compared to this fixed value. Many techniques are used to peg the in-cylinder

pressure probably the most convenient way is to measure the intake pressure with another pressure transducer and then make that inlet pressure equal to the in-cylinder pressure at intake bottom dead center IBDC equation 5 summarizes that procedure.

$$P_{cyl,bar} = P_{cyl,\ A/D\ converter} - P_{cyl,\frac{A}{D}converter\ at\ BDC} + P_{intake,BDC} \qquad (5)$$

In the following section we introduce the procedure to find the heat release rate inside the cylinder.

A.3 Cylinder volume

As mentioned before, pressure measurements are registered at specific crank angles depending on the encoder resolution. Knowing the in cylinder pressure plays a vital role to determine the in cylinder temperature as well as the heat release rate. The cylinder volume can simply be found by investigating the geometry of the crank slider mechanism. The formula of cylinder volume is given by equation 6 and is given here without derivation.

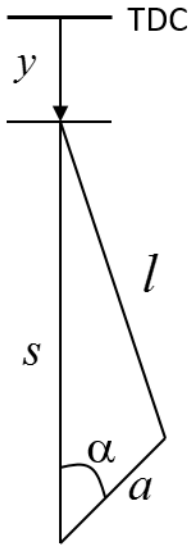

Figure 23: geometry of the crank slider mechanism

$$V(\alpha) = V_c + \frac{\pi\, B^2}{4}\, y(\alpha) \qquad (6)$$

Where

$V(\alpha)$ is the cylinder volume as a function of crank angle degree.

V_c is the clearance volume

B is the cylinder bore

$y(\alpha) = l + (1 - \cos\alpha)a - (l^2 - a^2 \sin^2\alpha)^{1/2}$, l and a are given as shown in figure 23.

In the next section we develop the heat release equation and then we comment on the heat losses and proposed models to approximate such losses.

A.4 Heat release

Heat release plays a vital role in studying the combustion inside an engine. The most important information given by the heat release rate is the fuel reactivity and the combustion phasing. Highly reactive fuels tends to burn way faster that less reactive fuels. This could be easily observed by studying the heat release behavior inside the cylinder. This section has two subsections. The first one gives the heat release equation derived from the first law of thermodynamics and the second section entitled “Heat losses” highlights the importance of modeling heat losses and the model used during this research.

A.4.1 Heat release equation

The derivation of the heat release equation depends on the first law of thermodynamics. Starting from

$$dQ = dU + dW \tag{6}$$

$$dQ = dQ_{hr} - dQ_{ht} - dQ_{cr} - dQ_{BL} \tag{7}$$

$$dU = \frac{C_v}{R}(VdP + PdV) \tag{8}$$

$$dW = PdV \tag{9}$$

$$C_p - C_v = R \tag{10}$$

$$\gamma = \frac{C_p}{C_v} \tag{11}$$

Combining these equation we get:

$$dQ_{hr} = \frac{\gamma}{\gamma - 1}PdV + \frac{1}{\gamma - 1}VdP + dQ_{ht} + dQ_{cr} \tag{12}$$

Or if we take it per crank angle degree we get:

$$\frac{dQ_{hr}}{d\theta} = \frac{\gamma}{\gamma - 1} P \frac{dV}{d\theta} + \frac{1}{\gamma - 1} V \frac{dP}{d\theta} + \frac{dQ_{ht}}{d\theta} + \frac{dQ_{cr}}{d\theta} \quad (13)$$

A.4.2 Heat losses

Some of the heat released during the combustion of fuel is lost in many forms. Those forms are mainly heat transfer, crevice losses, and blow-by losses. The major losses are the heat transfer losses in which heat is transferred to the surrounding medium due to the temperature difference. Since those losses are the main losses, it is customary among engine researchers to account for only heat transfer losses. Many models have been introduced to model heat transfer losses. One of those models is Wochni's heat transfer model which is widely used in engine community. Wochni's model has gained its popularity since it depends on easily measured physical quantities. This model only depends on measuring the in-cylinder pressure and then estimating the heat losses by adjusting some parameters that are different for different engines. The right parameters can be found by trial-and-error until zero heat release is achieved during motored cycles. The details and fluid dynamics behind this model are beyond the scope of this thesis. Thus, the model is stated here without detailed information. Table 5 states the symbols used in this model.

Table 5: symbols in the heat transfer losses model

$c, c_1, and\ c_2$	Constants that are unique for each engine and they must be tuned to have zero heat release at motoring.
w	Fluid velocity
s	The mean piston speed
V_d	Displacement volume
P_{cyl}	In-cylinder pressure
P_{mot}	Motored pressure
P_{ivc}	Pressure at intake valve closing
T	In-cylinder temperature
h	Heat transfer coefficient
B	Cylinder bore
A_w	Cylinder wall area

The fluid velocity w is found by the following equation

$$w = c_1 s + c_2 \left(\frac{V_d}{V_{ivc}}\right)\left(\frac{P_{cyl} - P_{mot}}{P_{cyl,ivc}}\right) T_{ivc,ivc} \quad (14)$$

$$h = c\ B^{-0.2}\ P_{cyl}^{0.8}\ T_{cyl}^{-0.55}\ w^{0.8} \quad (15)$$

Heat transfer rate per crank angle degree can thus be found using the following equation:

$$\frac{dQ_{ht}}{d\theta} = hA_w \frac{T_{cyl} - T_{wall}}{N\frac{360}{60}} \quad (16)$$

Where T_{wall} is the cylinder wall temperature and it is customary to assume it to be 100 $°C$. Also, N is the engine speed in rpm.

So far we have discussed the heat transfer losses only. As mentioned before, other losses are also present. Crevice losses account for the unburned hydrocarbons trapped in the cylinder crevices. Another type is blow-by losses which is simply the burned gases that escape the cylinder during the power stroke. These two losses are usually small compared to heat transfer losses and hence they are usually neglected. It is worth mentioning that model used in this research neglected such losses.

Appendix B: Efficiency Analysis

B.1 Introduction

The main goal of this research is to study the effect of increasing the specific heat ratio on the thermodynamic efficiency of the engine and hence the overall efficiency. This chapter explains the procedure used to study the engine efficiency. The chapter begins by introducing the concept of mean effective pressure. It then discusses the definitions of the different efficiencies that define the overall engine efficiency.

B.2 Mean effective pressure

Mean effective pressure (MEP) can be simply defined as work normalized by engine displacement. Hence the name pressure since it has the same units. It is convenient to report the mean effective pressure in bar since it is easy to be compared to atmospheric pressure that is approximately 1 bar. Figure 24 shows the different mean effective pressures inside the engine.

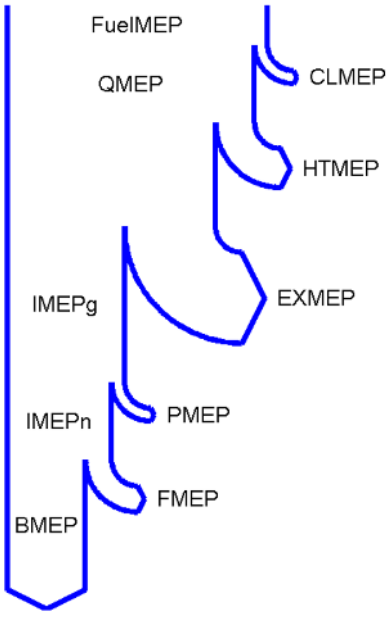

Figure 24: Energy flow in the internal combustion engine

The acronyms in figure 24 are is defined in the next table.

Table 6: Definitions of the different mean effective pressures

Acronym	Full name	Definition (All energies are normalized by engine displacement)
FuelMEP	Fuel MEP	Supplied fuel energy.
CLMEP	Combustion losses MEP	Energy of Elements in the exhaust that could have been burned.
QMEP	Released heat MEP	Amount of heat released by burning the fuel in the cylinder.
HTMEP	Heat transfer losses MEP	Amount of heat lost to the surroundings as a results of heat transfer due to temperature difference.
EXMEP	Exhaust losses MEP	The enthalpy of exhaust. Sometimes, these losses are utilized to drive engine turbocharger.
IMEPg	Gross indicated MEP	IMEPg = QMEP - EXMEP - EXMEP
PMEP	Pumping losses MEP	This is the part of gross indicated MEP that is lost as work done by the piston to pump the exhaust out of the cylinder.
IMEPn	Net Indicated MEP	IMEPn = IMEPg - PMEP
FMEP	Friction losses MEP	Mechanical Energy lost due to friction inside the engine
BMEP	Brake MEP	Total energy obtained from the engine.

Mean effective pressures play a vital role in determining different efficiencies. Next section uses mean effective pressures to have expressions for combustion, thermodynamic, gas exchange, and mechanical efficiencies.

B.3 Efficiency definitions

B.3.1 Combustion efficiency

The amount of fuel supplied to an internal combustion engine is not burned entirely. In fact, some of the fuel is trapped in the piston crevices. Thus, Combustion efficiency could be defined as the percentage of supplied fuel that burns inside the engine. For example, 90% combustion efficiency means that 90% of the supplied fuel is burned. A typical value for SI combustion efficiency is approximately 90%. This value increases in diesel engine to be as high as 98% percent [34]. Combustion efficiency can be estimated by conducting an exhaust analysis. The following equation can be used to estimate the combustion efficiency η_c:

$$\eta_c = 1 - \frac{\Sigma \frac{M_i}{M_p} x_i Q_{LHV,i}}{\frac{1}{1 + A/F}\ Q_{LHV,f}} \tag{17}$$

Where

M_i is the molar mass of species i

M_p is the molar mass of fuel

x_i is the mole fraction of species i

Q_{LHV} is the mole fraction of either fuel or species I

A/F mass air fuel ratio

Species i are mainly three species. That is Carbon monoxide, hydrocarbons, and hydrogen. It is also worth mentioning that experiments were conducted in a variable compression CFR engine that was equipped with an FTIR to perform an exhaust analysis and to find the combustion efficiency. It is not possible to detect diatomic molecules using FTIR analysis because of the zero dipole change. Expensive hydrogen sensors is thus needed to determine the amount of the hydrogen in the exhaust. Alternatively, water gas equation can be used to estimate the hydrogen concentration as follows:

$$x_{H_2} = \frac{x_{CO} x_{H_2O}}{K\ x_{CO_2}} \tag{18}$$

Where K is the water gas constant that is usually assumed to be 3.5.
Finally, combustion efficiency can be expressed in terms of mean effective pressures as follows:

$$\eta_c = \frac{QMEP}{FuelMEP} = \frac{FuelMEP - CLMEP}{FuelMEP} = 1 - \frac{CLMEP}{FuelMEP} \quad (19)$$

B.3.2 Thermodynamic efficiency

This is the efficiency that determines how much of the heat released is converted to mechanical work on the piston. As discussed previously, $QMEP$ could be calculated by knowing the combustion efficiency. Thermodynamic efficiency is then calculated using equation 20.

$$\eta_{th} = \frac{IMEP_g}{QMEP} \quad (20)$$

Where IMEPg could be easily calculated by finding the P-V work as shown in equation 21.

$$IMEP_g = \frac{1}{V_D} \int_0^{360} PdV \quad (21)$$

Sometimes heat transfer losses and exhaust losses need to be separated. In this case equation 22 estimates EXMEP as the enthalpy of the exhaust leaving the cylinder.

$$EXMEP = \frac{mc_p(T_{exh} - T_{amb})}{V_D} \quad (22)$$

Thus,

$$HTMEP = QMEP - EXMEP - IMEP_g \quad (23)$$

B.3.3 Gas exchange efficiency

Part of the mechanical work exerted on the piston is used to pump the exhaust out of the engine. Note that this is the case if intake pressure is lower than exhaust pressure. For this reason, boosted engine with elevated intake pressure could have a gas exchange efficiency exceeding unity. This should not be surprising since boosting the engine takes up some energy from the engine. For example, a turbocharger utilizes some of the exhaust energy to boost the intake pressure. Gas exchange efficiency is calculated using equation 24.

$$\eta_{ge} = \frac{IMEP_n}{IMEP_g} \quad (24)$$

An expression for $IMEP_g$ has been developed in the previous section. A similar expression exists for $IMEP_n$ the only difference is that pressure is integrated over the entire cycle.

$$IMEP_n = \frac{1}{V_D}\int_0^{720} PdV \tag{25}$$

B.3.4 Mechanical efficiency

Friction losses are part of any mechanical machine and internal combustion engines are no exception. It is worth mentioning that higher in-cylinder pressure means higher friction losses due to excessive loads on bearings increasing the friction losses. Equation 26 shows the mechanical efficiency based on mean effective pressures.

$$\eta_m = \frac{BMEP}{IMEP_g} \tag{26}$$

BMEP is found by measuring the work output of an engine by a dynamometer and then normalizing that work by the engine displacement.
Finally, overall engine efficiency is called brake efficiency and it is simply the product of all 4 efficiencies.

$$\eta_b = \eta_c \eta_{th} \eta_{ge} \eta_m \tag{27}$$

It can be easily noticed that the game of increasing the engine efficiency is not an easy one. Increasing one of those efficiencies usually results in decreasing other efficiencies. A viable engine efficiency solution optimizes those four efficiencies simultaneously.

Appendix C: Fourier transform infra-red (FTIR) exhaust Analysis

C.1 Introduction

Fourier transform infra-red (FTIR) is a chemical analysis technique that is widely used to analyze chemical samples. It has gained its popularity among internal combustion engine researchers due to its simplicity and acceptable accuracy. Despite being used in many engine laboratories around the world, many people in engine community does not fully understand what is behind this powerful technique. For this reason, the author decided to include this chapter in the appendix to highlight some of the important aspects of that technique. However, this chapter highlights the main aspects of this technique and the physics associated with analytical tool.

C.2 Theory of operation

Each gas molecule in a gas sample exposed to an infra-red radiation absorbs radiation of a certain wavelength. For example, CO2 absorbs radiation with different wavelength than radiation absorbed by NO2. This is the basic physical phenomenon that is utilized for the development of the FTIR analyzer.

In principle an FTIR analyzer works as follows: First, an inert solid material is excited by an electric heater to emit a wide infrared spectrum. The spectrum is then modulated in an interferometer. Next, the modulated spectrum is passed through the sample gas. Different molecules in this sample gas absorb IR radiation of a special wavelength. For example, CO will absorb radiation with a wavelength different than that absorbed by CO2. Thus, the absorption spectrum gives information about the molecules present in the sample. Unfortunately, despite being a powerful analytical tool, FTIR spectrometer cannot detect diatomic gases such as O2 and H2. The reason is that those molecules have zero dipole change in their vibrational and rotational patterns and hence they are not excited by the IR radiation.

C.3 Experimental setup and methodology

Previous section highlighted the main steps in finding gas concentrations in a gas sample. In this section we focus on the experimental setup used for this purpose. FTIR analyzer consists of five major parts: Gas sampling equipment, the IR emitting source, the interferometer, the detector, and finally a computer to process data.

A sample of the exhaust gas is firstly captured and routed to the chamber where it is exposed to a wide spectrum of IR radiation. This spectrum is generated by heating special solid inert materials to certain temperature until it emits the desired IR spectrum. IR radiation spectrum is modulated in a device called interferometer shown in figure 25. Modulation means that the signal is physically processed to measure the wavelength.

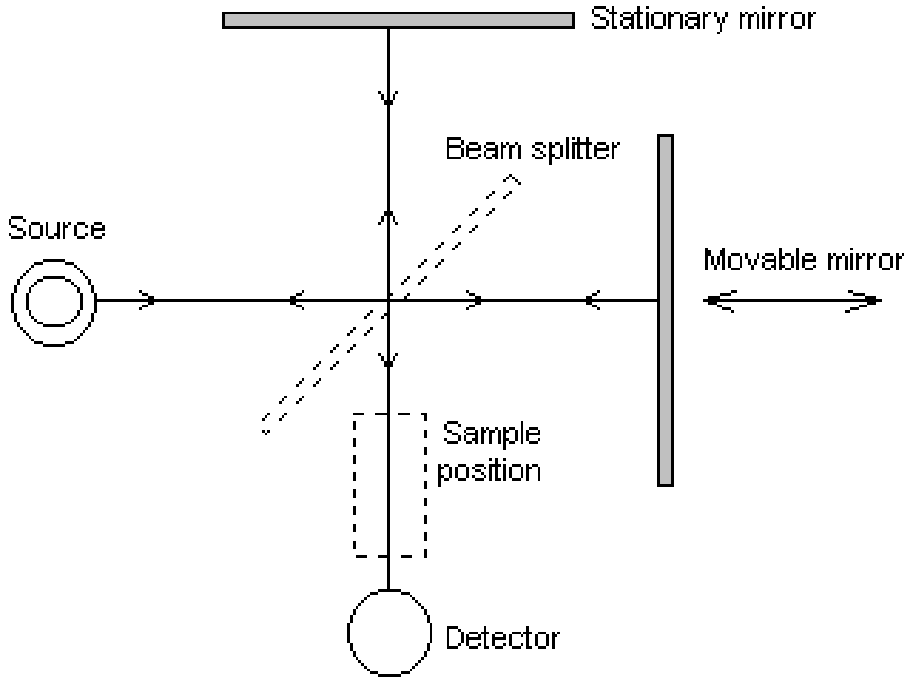

Figure 25: basic interferometer setup

The source emits a wide spectrum of IR radiation with different wavelengths. The moveable mirror starts to move back and forth and the detector will detect high intensity radiation from the gas sample at zero path difference (ZPD). Figure 26 shows a typical detector response in time domain (or optical wave length) and its Fourier transform. Fast Fourier transform FFT transforms that signal from time domain back to the frequency domain which means we can know the wavelengths present in the signal.

So far we know the different wavelengths present in the sample and its intensity. This profile that we have shown in figure 26 should be compared to the wavelengths detected when the sample gas is not present i.e. when the modulated signal is just passed to the detector without any sample gas present. This comparison will reveal what are the wavelengths absorbed by the sample gas. Figure 27 shows an example of the IR absorption spectrum obtained by the aforementioned comparison. Note that transmittance less than 100% means that part of the emission is absorbed.

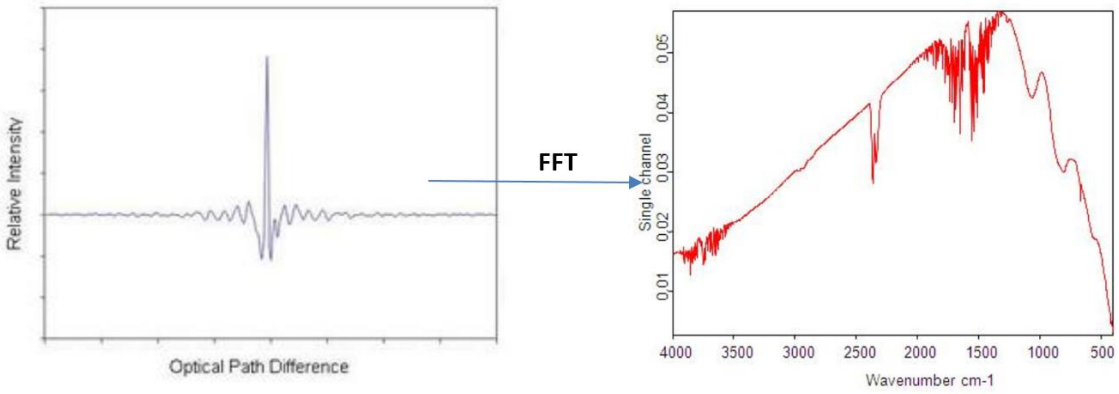

Figure 26: Fourier transform from time domain to frequency domain

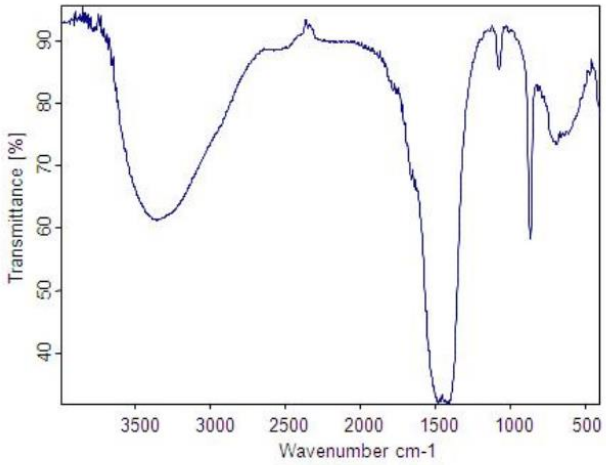

Figure 27: Transmittance IR spectrum

It can be easily noticed that around 70% of IR radiation with wavenumber 1500 cm^{-1} is absorbed and only 30% is transmitted. This means that the sample has a CH2 bend functional group since it absorbs that wavelength. A carefully designed computer program can easily do that process and provide the user with detailed information about the gases present in the sample.

Finally it is worth mentioning that the exhaust emissions were measured in this research using an AVL SESAM i60 FTIR analyzer. This equipment uses a spectrometer made by ThermoFisher scientific. The spectrum is analyzed using a built-in software that gives 25 species including pollutants controlled by law that is UHC, NOx, and CO. Other exhaust emission such as water vapor and CO2 concentrations can also be obtained.

Appendix D: Matlab program

D.1 Description

The results obtained in this thesis were generated by processing the experimental data in a MATLAB program. We begin this section by a quick overview of the main parts of that code. This code does three main tasks. The first one is to analyze the pressure measurements and the associated heat release analysis. Secondly, the code process the data obtained from the FTIR emission analyzer. Finally, it does a complete efficiency analysis to estimate combustion efficiency, thermodynamic efficiency, and gas exchange efficiency. The code relied on many assumptions that are stated in the next section. The code written in MATLAB programming language concludes this appendix.

D.2 Assumptions

The author of this thesis has attended a course by his advisor Professor Bengt Johansson in which the professor stated that “in heat release analysis everything is wrong, the question is only how bad it is!”. This highlights the importance of approximation and educated assumptions made during the analysis of the engine results. Here we state the main assumption made in writing the code. It is worth noting that those are not all the assumptions. There might be other assumptions made during the actual programming. However, the results obtained were compared to results obtained by other codes and they showed an acceptable agreement.

D.2.1 Pegging In-cylinder pressure

The term pegging has been already introduced in heat release analysis chapter. To peg the pressure signal the in-cylinder pressure was assumed to be equal to the intake pressure at intake valve closing. This is a reasonable assumption since the cylinder is already filled with the working fluid and the pressure should be balanced with the intake. Other pressure measurements were then adjusted based on this assumption.

D.2.2 Ideal gas law to find in-cylinder temperature

Cheap and handy thermocouples are of no use in measuring the in-cylinder temperature. The relatively high temperature will burn the thermocouple immediately and we can have the in-cylinder temperature for just one engine cycle. For this reason, it is convenient to estimate the temperature by the ideal gas law since information of pressure and volume is available. Real gases tend to behave ideally at low densities i.e. at high temperature and low pressures. In-cylinder temperature is relatively high and pressure is no exception. Compressibility factor Z is a popular way among scientists to correct the ideal gas law.

$$Z = \frac{PV}{RT} \tag{28}$$

The highest in-cylinder pressure obtained during experiments does not exceed 80 bar. With an average of around 1700 K with air as the working fluid, we can find reduced pressure $P_r \approx 2$ and reduced temperature $T_r \approx 13$. With these values it can be seen from the generalized compressibility chart (figure 28) that compressibility factor Z is almost unity and we can assume the ideal behavior with a an error of less than 3%.

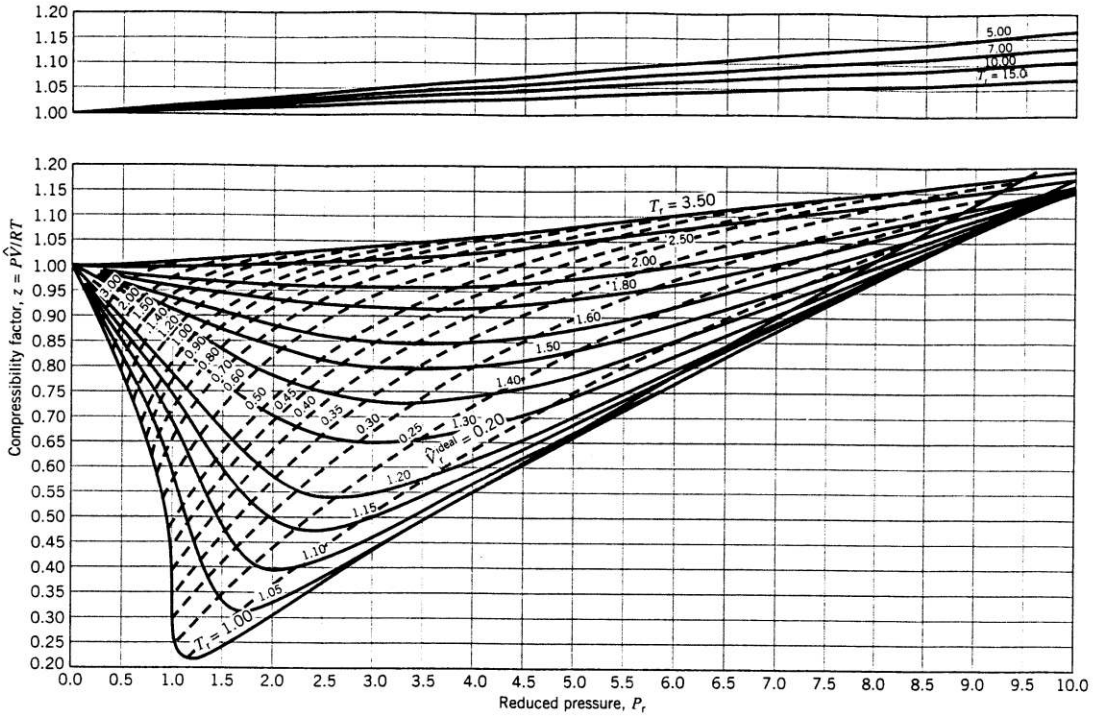

Figure 28: Generalized compressibility chart [35]

D.2.3 Specific heat ratio approximation

Specific heats are a function of temperature in real gases. It thus important to make the specific heat ratio of the mixture dependent on temperature. The temperature dependence could be easily modeled using NASA's polynomial fits as shown in equation 29.

$$\frac{c_p(T)}{R} = a_1 + a_2T + a_3T^2 + a_4T^3 + a_5T^4 \quad (29)$$

c_p is the specific heat at constant pressure, R is the ideal gas constant, T is the temperature, and the coefficients a_1 , a_2 , a_3 , a_4 , a_5 are coefficients taken from Burcat's tables [29].

The real challenge in estimating the specific heat ratio is that we have a reacting mixtures in which reactants and products have different specific heat ratios. It was assumed that the mixture consists of all reactants before top dead center and all reactants after top dead center. This a reasonable assumption since HCCI combustion is a relatively fast combustion process. More accurate model should utilize advanced chemical kinetics.

D.2.4 Total hydrocarbon approximation

Combustion efficiency is a strong function of the amount of hydrocarbons present in the exhaust. Higher unburned hydrocarbons in the exhaust means poor combustion efficiency consequently deteriorating the engine brake efficiency. Total unburned hydrocarbons is usually measured more accurately by a flame ionization detector (FID). However, the FTIR analyzer was used to estimate the total hydrocarbons in these experiments. There is no universal formula for all FTIR analyzers to estimate the total hydrocarbons. After a literature review we used the following formula to estimate this value [36].

$$UHC = CH_4 + 2C_2H_2 + 2C_2H_4 + 3C_3H_6 + 5IC_5 + 5NC_5 + 7.5AHC \quad (30)$$

Table 7 shows the full names for the abbreviations and molecular formulae found in the previous equation.

Table 7: Unburned hydrocarbons and their abbreviations/ molecular formulae

Abbreviation \ molecular formula	Compound name
UHC	Total unburned hydrocarbons
CH_4	Methane
C_2H_2	Acetylene
C_2H_4	Ethylene
C_3H_6	Propane
IC_5	Isopentane
NC_5	Normal pentane
AHC	Aromatic hydrocarbons

D.3 Code

```
%--------------------------------------------------------------------------
%       Heat relese code for the CFR experiments
%       Written by: Magdy
%       27/April/2018
%--------------------------------------------------------------------------
%clear all
%close all
%--------------------------------------------------------------------------
%                               Engine specs
%--------------------------------------------------------------------------
bore = 82.55/1000; %bore in m
stroke = 114.3/1000; %stroke in m
connecting_rod = 256/1000; %conncting rod length in m
radius = stroke/2; %radius of the crank shaft in m
%--------------------------------------------------------------------------
%                            mean piston speed
%--------------------------------------------------------------------------
N = 600; %rpm
mean_piston_speed = 2*N/60*stroke;
%--------------------------------------------------------------------------
%           reading the parameters and the cycles files
%--------------------------------------------------------------------------
%---------------------------------
%first read the parameters file
%---------------------------------
[name path] = uigetfile('*parameters*.txt','choose parameters file');
name = strcat(path,name);
parameters_file = fopen(name);
%get the number of columns
line = fgetl(parameters_file);
headers = textscan(line,'%s','delimiter','\t');
no_columns_parameters = length(headers{1});
```

```
form = '%f';
i = 1;
for i = 1 : no_columns_parameters-1
    form = [form ' %f'];
    i = i+1;
end
fclose(parameters_file);
%read the data from the file
parameters_file = fopen(name);
parameters_data = textscan(parameters_file,form,'HeaderLines',1);
compression_ratio = parameters_data{49}; %compression ratios 200 cycles
compression_ratio = mean(compression_ratio); %take the mean of the compression ratios
intake_temperature = parameters_data{36}; %Get the intake temperatures
exhaust_temperature = parameters_data{38}; %Get the exhaust temperature
room_temperature = parameters_data{33}; %Get the room temperature
phi = parameters_data{50}; %equivelance ratio
phi = mean(phi); %take the mean of the equivelance ratio
fuel_flow = mean(parameters_data{52}); %Take the mean of fuel flow
fuel_density = mean(parameters_data{53}); %Take the mean of fuel Density
fclose(parameters_file);
%--------------------------------
%second read the cycles file
%--------------------------------
[name path] = uigetfile('*cycles*.txt','choose cycles file');
name = strcat(path,name);
cycles_file = fopen(name);
%get the number of columns
line = fgetl(cycles_file);
headers = textscan(line,'%s','delimiter','\t');
no_columns_cycles = length(headers{1});
form = ' %f';
i = 1;
for i = 1 : no_columns_cycles-1
    form = [form '%f'];
    i = i+1;
end
fclose(cycles_file);
%read the data from the file
cycles_file = fopen(name);
cycles_data = textscan(cycles_file,form,'HeaderLines',1);
CA = cycles_data{1}; %Crank angle
Pcyl = cycles_data{2}; %Presure transducer reading
Pin = cycles_data{3}; %intake pressure
Pex = cycles_data{4}; %exhaust pressure
PMEP = mean(Pex)-mean(Pin);
fclose(cycles_file);
%--------------------------------
%Third read the emmissions file
%--------------------------------
[name path] = uigetfile('*Pollutants*.txt','choose emmissions file');
name = strcat(path,name);
emmission_file = fopen(name);
%get the number of COlumns
line = fgetl(emmission_file);
headers = textscan(line,'%s','delimiter','\t');
no_COlumns_emmission = length(headers{1});
form = '%f';
i = 1;
for i = 1:no_COlumns_emmission-1
    form = [form ' %f'];
    i = i+1;
end
fclose(emmission_file);
%read the data from the file
emmission_file = fopen(name);
emmission_data = textscan(emmission_file,form,'HeaderLines',1);
NO = mean(emmission_data{1}); %nitrogen monoxide
H2O = mean(emmission_data{2}); %water
CH4 = mean(emmission_data{3}); %Methane
CO = mean(emmission_data{4}); %carbon monoxide
NO2 = mean(emmission_data{5}); %nitrogen dioxide
```

```
N2O = mean(emmission_data{6}); %Nitrous oxide
NH3 = mean(emmission_data{7}); %ammonia
SO2 = mean(emmission_data{8}); %sulfar dioxide
HCHO = mean(emmission_data{9}); %formaldyhyde
C2H2 = mean(emmission_data{10}); %Acetylene
C2H4 = mean(emmission_data{11}); %Ethylene
IC5 = mean(emmission_data{12});  %Isopentane
AHC = mean(emmission_data{13});  %taotal aromatics COncentration
C3H6 = mean(emmission_data{14}); %propane
C4H6 = mean(emmission_data{15}); %Butene
MECHO = mean(emmission_data{16});%Acetaldehyde
COS = mean(emmission_data{17}); %Carbonyl sulfide
NC5 = mean(emmission_data{18}); %Normal Pentane
C2H6 = mean(emmission_data{19}); %Ethane
MEOH = mean(emmission_data{20}); %Methanol
HCN = mean(emmission_data{21});  %hydrogen cyanide
ETOH = mean(emmission_data{22}); %Ethanol
CO2 = mean(emmission_data{23}); %carbon dioxide
HCG = mean(emmission_data{24}); %Hydrocarbon gas
NOx = mean(emmission_data{25}); %total NOx
NMHC = mean(emmission_data{26}); %Non-methane HydroCarbons
RATIO = mean(emmission_data{27});
fclose(emmission_file); %close file
%--------------------------------------------------------------------------
%                    gamma and density of the mixture
%--------------------------------------------------------------------------
%gases are assumed to behave ideally with mass fraction averaging
% The program is designed to process dual gas mixture
prompt = {'choose Air=1, Nitrogen=2, Argon=3'};
title = '';
answer = inputdlg(prompt,title);
check = str2num(answer{1});
%--------------------------------------------------------------------------
%                                 Volume
%--------------------------------------------------------------------------
%We have to find the volume as a function of CAD
%volume is important for heat release calculations
CA = CA(1:3600); %only 3600 angles
CA_rad = degtorad(CA);
y = connecting_rod+(1-cos(CA_rad))*radius-sqrt(connecting_rod^2-...
    radius^2*sin(CA_rad).^2);
displaced_volume = 0.25*pi*bore^2*stroke;
clearance_volume = displaced_volume / (compression_ratio-1);
volume = clearance_volume  + 0.25*pi*bore^2*y;
%--------------------------------------------------------------------------
%                            Pressure trace
%--------------------------------------------------------------------------
%the method used to peg the pressure is very simple
%Intake pressure is assumed to be equal to the in-cylinder pressure when
%Intake valve closes (IVC) ... for the CFR IVC = -146 ATDC
Pcyl = reshape(Pcyl,3600,200);
Pin = reshape(Pin,3600,200);
%pegging
for i = 1:200
    Pcyl(1:3600,i) = Pcyl(1:3600,i) - Pcyl(1071,i) + Pin(1071,i);
end
Pcyl_mean = mean(Pcyl,2);
%plot in cylinder pressure
figure(1)
hold on
plot(CA,Pcyl_mean,'LineWidth',1)
xlim([-100 100])
ylim([0 80])
grid on
xlabel('CAD (ATDC)')
ylabel('In-cylinder pressure (bar)')
legend('Air, CR = 15 ','Nitrogen + O_2, CR = 15','Argon + O_2, CR = 8.8')
% plot P-V diagram
figure(2)
hold on
plot(volume*1000,Pcyl_mean,'LineWidth',1)
```

```
grid on
xlabel('Volume (L)')
ylabel('In-cylinder pressure (bar)')
legend('Air','Nitrogen + O_2','Argon + O_2')
figure(9)
hold on
plot(log(volume*1000),log(Pcyl_mean),'LineWidth',1)
grid on
xlabel('Log Volume [log(L)]')
ylabel('Log In-cylinder pressure [log(bar)]')
legend('Air','Nitrogen + O_2','Argon + O_2')
%--------------------------------------------------------------------------
%                          In-cylinder Temperature
%--------------------------------------------------------------------------
%this analysis is based on the ideal gas law PV = mRT
Tivc = intake_temperature+273.2+(exhaust_temperature-intake_temperature)...
    /(compression_ratio);
Tcyl = zeros(3600,200);
for i=1:200
    Tcyl(:,i) = Pcyl(:,i).*volume*Tivc(i)./Pcyl(1071,i)./volume(1071);
end
Tcyl_mean = mean(Tcyl,2);
figure(3)
hold on
plot(CA,Tcyl_mean,'LineWidth',1)
xlim([-100 100])
xlabel('CAD (ATDC)')
ylabel('Incylinder Temperature (K)')
grid on
legend('Air','Nitrogen + O_2','Argon + O_2')
%plot T-V diagram
figure(4)
hold on
plot(volume(900:2800)*1000,Tcyl_mean(900:2800),'LineWidth',1)
xlabel('Volume (L)')
ylabel('Incylinder Temperature (K)')
grid on
legend('Air','Nitrogen + O_2','Argon + O_2')
%--------------------------------------------------------------------------
%                gamma calculations using Burcat's Table
%--------------------------------------------------------------------------
R_u = 8.3145;
%initilize Cp & Cv
Cp_fuel = zeros(3600,1);
Cp_Ar= zeros(3600,1);
Cp_O2 = zeros(3600,1);
Cp_N2 = zeros(3600,1);
Cp_CO2 = zeros(3600,1);
Cp_H2O = zeros(3600,1);
Cp = zeros(3600,1);
%Mixture elements
%fuel
a = [1.76160941E+01 5.13323108E-02 -1.65307266E-05 2.43232275E-09 -1.35572757E-13 ...
-3.63461118E+04 -6.86446285E+01 8.15741071E-01 7.32647307E-02 1.78301503E-05 ...
-6.93592790E-08 3.21630852E-11 -3.04774255E+04 2.41511097E+01 -2.69420567E+04];
for i=1:3600
    if Tcyl_mean(i) >= 1000
    Cp_fuel(i) = R_u*(a(1)+a(2)*Tcyl_mean(i)+a(3)*Tcyl_mean(i)^2 ...
        +a(4)*Tcyl_mean(i)^3+a(5)*Tcyl_mean(i)^4);
    elseif Tcyl_mean(i) < 1000
    Cp_fuel(i) = R_u*(a(8)+a(9)*Tcyl_mean(i)+a(10)*Tcyl_mean(i)^2 ...
        +a(11)*Tcyl_mean(i)^3+a(12)*Tcyl_mean(i)^4);
    end
end
Cv_fuel = Cp_fuel - R_u;
%Argon
     a = [2.50000000E+00 0.00000000E+00 0.00000000E+00 0.00000000E+00 0.00000000E+00 ...
    -7.45375000E+02 4.37967491E+00 2.50000000E+00 0.00000000E+00 0.00000000E+00 ...
     0.00000000E+00 0.00000000E+00 -7.45375000E+02 4.37967491E+00 0.00000000E+00];
    for i=1:3600
        if Tcyl_mean(i) >= 1000
```

```
        Cp_Ar(i) = R_u*(a(1)+a(2)*Tcyl_mean(i)+a(3)*Tcyl_mean(i)^2 ...
            +a(4)*Tcyl_mean(i)^3+a(5)*Tcyl_mean(i)^4);
        elseif Tcyl_mean(i) < 1000
        Cp_Ar(i) = R_u*(a(8)+a(9)*Tcyl_mean(i)+a(10)*Tcyl_mean(i)^2 ...
            +a(11)*Tcyl_mean(i)^3+a(12)*Tcyl_mean(i)^4);
        end
    end
    Cv_Ar = Cp_Ar - R_u;
%oxygen
a = [3.66096065E+00 6.56365811E-04 -1.41149627E-07 2.05797935E-11 -1.29913436E-15 ...
-1.21597718E+03 3.41536279E+00 3.78245636E+00 -2.99673416E-03 9.84730201E-06 ...
-9.68129509E-09 3.24372837E-12 -1.06394356E+03 3.65767573E+00 0.00000000E+00];
    for i=1:3600
        if Tcyl_mean(i) >= 1000
        Cp_O2(i) = R_u*(a(1)+a(2)*Tcyl_mean(i)+a(3)*Tcyl_mean(i)^2 ...
            +a(4)*Tcyl_mean(i)^3+a(5)*Tcyl_mean(i)^4);
        elseif Tcyl_mean(i) < 1000
        Cp_O2(i) = R_u*(a(8)+a(9)*Tcyl_mean(i)+a(10)*Tcyl_mean(i)^2 ...
            +a(11)*Tcyl_mean(i)^3+a(12)*Tcyl_mean(i)^4);
        end
    end
    Cv_O2 = Cp_O2 - R_u;
%Nitrogen
a = [2.95257637E+00 1.39690040E-03 -4.92631603E-07 7.86010195E-11 -4.60755204E-15 ...
-9.23948688E+02 5.87188762E+00 3.53100528E+00 -1.23660988E-04 -5.02999433E-07 ...
 2.43530612E-09 -1.40881235E-12 -1.04697628E+03 2.96747038E+00 0.00000000E+00];
    for i=1:3600
        if Tcyl_mean(i) >= 1000
        Cp_N2(i) = R_u*(a(1)+a(2)*Tcyl_mean(i)+a(3)*Tcyl_mean(i)^2 ...
            +a(4)*Tcyl_mean(i)^3+a(5)*Tcyl_mean(i)^4);
        elseif Tcyl_mean(i) < 1000
        Cp_N2(i) = R_u*(a(8)+a(9)*Tcyl_mean(i)+a(10)*Tcyl_mean(i)^2 ...
            +a(11)*Tcyl_mean(i)^3+a(12)*Tcyl_mean(i)^4);
        end
    end
    Cv_N2 = Cp_N2 - R_u;
%CO2
a = [0.46365111E+01 0.27414569E-02 -0.99589759E-06 0.16038666E-09 -0.91619857E-14 ...
-0.49024904E+05 -0.19348955E+01 0.23568130E+01 0.89841299E-02 -0.71220632E-05 ...
 0.24573008E-08 -0.14288548E-12 -0.48371971E+05 0.99009035E+01 -0.47328105E+05];
    for i=1:3600
        if Tcyl_mean(i) >= 1000
        Cp_CO2(i) = R_u*(a(1)+a(2)*Tcyl_mean(i)+a(3)*Tcyl_mean(i)^2 ...
            +a(4)*Tcyl_mean(i)^3+a(5)*Tcyl_mean(i)^4);
        elseif Tcyl_mean(i) < 1000
        Cp_CO2(i) = R_u*(a(8)+a(9)*Tcyl_mean(i)+a(10)*Tcyl_mean(i)^2 ...
            +a(11)*Tcyl_mean(i)^3+a(12)*Tcyl_mean(i)^4);
        end
    end
    Cv_CO2 = Cp_CO2 - R_u;
%water vapor
a = [0.26770389E+01 0.29731816E-02 -0.77376889E-06 0.94433514E-10 -0.42689991E-14 ...
-0.29885894E+05 0.68825500E+01 0.41986352E+01 -0.20364017E-02 0.65203416E-05 ...
-0.54879269E-08 0.17719680E-11 -0.30293726E+05 -0.84900901E+00 -0.29084817E+05];
    for i=1:3600
        if Tcyl_mean(i) >= 1000
        Cp_H2O(i) = R_u*(a(1)+a(2)*Tcyl_mean(i)+a(3)*Tcyl_mean(i)^2 ...
            +a(4)*Tcyl_mean(i)^3+a(5)*Tcyl_mean(i)^4);
        elseif Tcyl_mean(i) < 1000
        Cp_H2O(i) = R_u*(a(8)+a(9)*Tcyl_mean(i)+a(10)*Tcyl_mean(i)^2 ...
            +a(11)*Tcyl_mean(i)^3+a(12)*Tcyl_mean(i)^4);
        end
    end
    Cv_H2O = Cp_H2O - R_u;
%Fuel Properties
a_c = 8;
b_h = 18;
a_th = a_c+b_h/4;
if check == 1
    %air
    n_tot_r = 1+a_th/phi+3.773*a_th/phi;
```

```
    n_tot_p = a_c+b_h/2+3.773*a_th/phi+a_th/phi-a_c-b_h/2;
    Cp(1:1800) = (1/n_tot_r).*Cp_fuel(1:1800)+(a_th/phi/n_tot_r).*Cp_O2(1:1800) ...
        + (a_th*3.773/phi/n_tot_r).*Cp_N2(1:1800);
    Cp(1801:3600) = (a_c/n_tot_p).*Cp_CO2(1801:3600)+(b_h/2/n_tot_p)*Cp_H2O(1801:3600)
...
        + (a_th*3.773/phi/n_tot_p).*Cp_N2(1801:3600) + ((a_th/phi-a_c-
b_h/4)/n_tot_p).*Cp_O2(1801:3600);
    Cv = Cp - R_u;
    gamma = Cp./Cv;
    M_m_r = (1/n_tot_r)*(8*12+18)+(a_th/phi/n_tot_r)*(32) ...
        + (a_th*3.773/phi/n_tot_r)*(28);
   elseif check == 2
    %Nitrogen
    n_tot_r = 1+a_th/phi+4*a_th/phi;
    n_tot_p = a_c+b_h/2+4*a_th/phi+a_th/phi-a_c-b_h/2;
    Cp(1:1800) = (1/n_tot_r).*Cp_fuel(1:1800)+(a_th/phi/n_tot_r).*Cp_O2(1:1800) ...
        + (a_th*4/phi/n_tot_r).*Cp_N2(1:1800);
    Cp(1801:3600) = (a_c/n_tot_p).*Cp_CO2(1801:3600)+(b_h/2/n_tot_p)*Cp_H2O(1801:3600)
...
        + (a_th*4/phi/n_tot_p).*Cp_N2(1801:3600) + ((a_th/phi-a_c-
b_h/4)/n_tot_p).*Cp_O2(1801:3600);
    Cv = Cp - R_u;
    gamma = Cp./Cv;
    M_m_r = (1/n_tot_r)*(8*12+18)+(a_th/phi/n_tot_r)*(32) ...
        + (a_th*4/phi/n_tot_r)*(28);
   elseif check == 3
    %Argon
    n_tot_r = 1+a_th/phi+4*a_th/phi;
    n_tot_p = a_c+b_h/2+4*a_th/phi+a_th/phi-a_c-b_h/2;
    Cp(1:1800) = (1/n_tot_r).*Cp_fuel(1:1800)+(a_th/phi/n_tot_r).*Cp_O2(1:1800) ...
        + (a_th*4/phi/n_tot_r).*Cp_Ar(1:1800);
    Cp(1801:3600) = (a_c/n_tot_p).*Cp_CO2(1801:3600)+(b_h/2/n_tot_p)*Cp_H2O(1801:3600)
...
        + (a_th*4/phi/n_tot_p).*Cp_Ar(1801:3600) + ((a_th/phi-a_c-
b_h/4)/n_tot_p).*Cp_O2(1801:3600);
    Cv = Cp - R_u;
    gamma = Cp./Cv;
    M_m_r = (1/n_tot_r)*(8*12+18)+(a_th/phi/n_tot_r)*(32) ...
        + (a_th*4/phi/n_tot_r)*(39.948);
end
gamma_mean = mean(gamma);
%plotting Gamma
figure(5)
hold on
plot(CA,gamma,'LineWidth',1)
xlim([-360 360]);
ylabel('Specific heat ratio C_p/C_v')
xlabel('CAD (ATDC)')
grid on
legend('Air','Nitrogen + O_2','Argon + O_2')
plot(CA,gamma_mean*ones(length(CA),1),'--')
%--------------------------------------------------------------------------
%                           Motored Pressure Estimated
%--------------------------------------------------------------------------
Pmot = zeros(3600,1); %initilize
Pmot(1:1780) = Pcyl_mean(1:1780);
Pmot(1781:2501) = (volume(1781)./volume(1781:2501)).^gamma(1781:2501).*Pcyl_mean(1781);
Pmot(2502:3600) = Pmot(2501);
%--------------------------------------------------------------------------
%                              Wochni Heat losses
%--------------------------------------------------------------------------
c = 131; % Woschni Coefficients
c1 = 2.28;
c2 = 2.4E-3;
w = c1*mean_piston_speed+c2*(displaced_volume/volume(1071))*...
    ((Pcyl_mean-Pmot)./Pcyl_mean(1071))*Tcyl_mean(1071); %velocity
h = c*bore^(-0.2)*Pcyl_mean.^(0.8).*Tcyl_mean.^(-0.55).*w.^(0.8); %heat transfer
coefficient
%----------------------------
% Surface Area
%----------------------------
```

```
A_w = 2*pi*bore^2/4+pi*bore*y;
T_wall = 373; %assumption
dQdCAD = h.*A_w.*(Tcyl_mean-T_wall)./(N*360/60);
%--------------------------------------------------------------------------
%                               Heat release
%--------------------------------------------------------------------------
grad_volume = gradient(volume,CA);
Pcyl = Pcyl*100000;
for i = 1:200
grad_pressure(:,i) = gradient(Pcyl(1:3600,i),CA);
end
for i = 1:200
HRR(:,i) = Pcyl(:,i).*grad_volume.*gamma./(gamma-1)+volume.*...
    grad_pressure(:,i)./(gamma-1);
end
HRR_mean = mean(HRR,2) + dQdCAD;
%plot Heat release rate
figure(6)
hold on
plot(CA,HRR_mean,'LineWidth',1);
xlim([-360 360]);
% ylim([-5 180]);
ylabel('Heat release rate (J/CAD)')
xlabel('CAD (ATDC)')
grid on
legend('Air','Nitrogen + O_2','Argon + O_2')
%refining HRR_mean
% for i=1:1750
%     HRR_mean(i) = 0;
% end
%
% for i = 1840:3600
%     HRR_mean(i) = 0;
% end
%--------------------------------------------------------------------------
%                               Accumlated Heat
%--------------------------------------------------------------------------
for i = 1072:2501
    Heat(i-1071) = trapz(CA(1070:i),HRR_mean(1070:i));
end
%plot accumlated heat
figure(7)
hold on
grid on
plot(CA(1072:2501),Heat,'LineWidth',1)
ylabel('Accumulated heat (J)')
xlabel('CAD (ATDC)')
legend('Air','Nitrogen + O_2','Argon + O_2')
%--------------------------------------------------------------------------
%--------------------------------------------------------------------------
%                       Efficiency analysis
%--------------------------------------------------------------------------
%--------------------------------------------------------------------------
%--------------------------------------------------------------------------
%                   combustion efficiency
%--------------------------------------------------------------------------
%%%%%%Hydrogen estimation
K = 3.5; %water gas constant
X_H2 = (CO/1E6)*(H2O/1E6)/(K*CO2/1E6);
%total hydrocarbons
UHC = CH4 + 2*C2H2 + 2*C2H4 + 3*C3H6 + 5*IC5 + 5*NC5 + 7.5*AHC; %Cite the reference
%stoichemtric F/A ratio
if check == 3
    F_A = (8*12+18)/(12.5*(32+4*39.948)); %Argon
elseif check == 1
    F_A = (8*12+18)/(12.5*(32+3.773*28));%air
elseif check == 2
    F_A = (8*12+18)/(12.5*(32+4*28)); %nitrogen
end
```

```
%molar masses
m_CH4 = 12+4; m_C2H2 = 12*2+2; m_C2H4 = 12*2+4; m_C3H6=3*12+6; m_C5 = 5*12+12; m_AHC =
78.11;
m_fuel = 8*12+18; m_CO = 12+16; m_H2 = 2.01588;
%LHV
LHV_CH4 = 50; LHV_C2H2 = 49.9; LHV_C2H4 = 47.2; LHV_C3H6 = 45.8; LHV_C5 = 44.9;
LHV_AHC = 41.8; LHV_fuel = 44.310;
LHV_CO = 10.1; LHV_H2 = 120;
%combustion efficiency
sigma = (m_CH4*CH4/1E6*LHV_CH4+m_C2H2*C2H2/1E6*LHV_C2H2+m_C2H4*C2H4/1E6*LHV_C2H4+...
    m_C3H6*C3H6/1E6*LHV_C3H6+m_C5*IC5/1E6*LHV_C5+m_C5*NC5/1E6*LHV_C5+...
    m_AHC*AHC/1E6*LHV_AHC+m_CO*CO/1E6*LHV_CO+m_H2*X_H2*LHV_H2)/(8*12+18);
AF = 1/(phi*F_A);
eta_c = 1-sigma/(LHV_fuel/(1+AF))
%Fuel mean effective pressure
n = Pcyl_mean(1802)*1E5*volume(1802)/(R_u*1E3)/Tcyl_mean(1802);
m = n*M_m_r;
FuelMEP = fuel_flow*fuel_density*LHV_fuel*1E6/(300*60*1000)/displaced_volume/1e5;
%Heat released mean effective pressure
QMEP = eta_c*FuelMEP;
%Approximation of the exhhaust losses
Delta_temperature = exhaust_temperature - room_temperature;
Delta_temperature = mean(Delta_temperature);
Qex = m*Cp*1000*Delta_temperature;
EXMEP = Qex/displaced_volume/1E5;
%IMEP calculations
IMEPg = (trapz(volume(1072:2501),Pcyl_mean(1072:2501)))/displaced_volume;
IMEPn = (trapz(volume,Pcyl_mean))/displaced_volume;
PMEP = IMEPg-IMEPn;
%thermodynamic efficiency
eta_th = IMEPg/QMEP
%gas exchange efficiency
eta_ge = IMEPn/IMEPg
%indicated efficiency
eta_in = eta_c*eta_th*eta_ge
%all MEP
CLMEP = FuelMEP-QMEP;
HTMEP = QMEP-EXMEP-IMEPg;
Magdy_check = Heat(end)/displaced_volume/1E5/QMEP*100
if check == 1
    QMEP_Wu = zeros(3,1);
    QMEP_Ex = zeros(3,1);
end
QMEP_Wu(check)=Heat(end)/displaced_volume/1E5;
QMEP_Ex(check)=QMEP;
if check==3
    figure(8)
    plot(QMEP_Wu,'-s','LineWidth',1.5);
    hold on
    grid on
    plot(QMEP_Ex,'-^','LineWidth',1.5);
    legend('Wuchni','Emission analysis')
%   title('QMEP Estimation')
    ylabel('QMEP [bar]')
    xticks([1 2 3])
    xticklabels({'Air','N_2+O_2','Ar+O_2'})
end
```